cmgh
CELLULAR AND MOLECULAR GASTROENTEROLOGY AND HEPATOLOGY

ORIGINAL RESEARCH

Microbiota-Inducible Innate Immune Siderophore Binding Protein Lipocalin 2 Is Critical for Intestinal Homeostasis

Vishal Singh,[1,*] Beng San Yeoh,[1,*] Benoit Chassaing,[2] Benyue Zhang,[2] Piu Saha,[1] Xia Xiao,[1] Deepika Awasthi,[3] Rangaiah Shashidharamurthy,[4] Madhu Dikshit,[3] Andrew Gewirtz,[2] and Matam Vijay-Kumar[1,5]

[1]*Department of Nutritional Sciences, The Pennsylvania State University, University Park, Pennsylvania;* [2]*Center for Inflammation, Immunity and Infection, Institute of Biomedical Sciences, Georgia State University, Atlanta, Georgia;* [3]*Pharmacology Division, Council of Scientific and Industrial Research-Central Drug Research Institute, Lucknow, India;* [4]*Department of Pharmaceutical Sciences, Philadelphia College of Osteopathic Medicine, Suwanee, Georgia;* [5]*Department of Medicine, The Pennsylvania State University Medical Center, Hershey, Pennsylvania*

SUMMARY

The current study identifies the role of lipocalin 2, a microbiota-inducible innate immune protein, in regulating intestinal homeostasis, and show that mice lacking lipocalin 2 harbor colitogenic microbiota and are susceptible to intestinal inflammatory disease.

BACKGROUND & AIMS: Lipocalin 2 (Lcn2) is a multifunctional innate immune protein whose expression closely correlates with the extent of intestinal inflammation. However, whether Lcn2 plays a role in the pathogenesis of gut inflammation is unknown. Herein, we investigated the extent to which Lcn2 regulates inflammation and gut bacterial dysbiosis in mouse models of IBD.

METHODS: Lcn2 expression was monitored in murine colitis models and upon microbiota ablation/restoration. Wild-type (WT) and *Lcn2* knockout (*Lcn2*KO) mice were analyzed for gut bacterial load, composition by 16S ribosomal RNA gene pyrosequencing, and their colitogenic potential by co-housing with interleukin (*Il*)*10*KO mice. Acute (dextran sodium sulfate) and chronic (IL10R neutralization and T-cell adoptive transfer) colitis were induced in WT and *Lcn2*KO mice with or without antibiotics.

RESULTS: Lcn2 expression was dramatically induced on inflammation and was dependent on the presence of a gut microbiota and MyD88 signaling. Use of bone marrow–chimeric mice showed that nonimmune cells are the major contributors of circulating Lcn2. *Lcn2*KO mice showed increased levels of *entA*-expressing gut bacteria burden, and, moreover, a broadly distinct bacterial community relative to WT littermates. *Lcn2*KO mice developed highly colitogenic T cells and showed exacerbated colitis on exposure to DSS or neutralization of IL10. Such exacerbated colitis could be prevented by antibiotic treatment. Moreover, exposure to the microbiota of *Lcn2*KO mice, via cohousing, resulted in severe colitis in *Il10*KO mice.

CONCLUSIONS: Lcn2 is a bacterially induced, MyD88-dependent protein that plays an important role in gut homeostasis and a pivotal role on challenge. Hence, therapeutic manipulation of Lcn2 levels may provide a strategy to help manage diseases driven by alteration of the gut microbiota. *(Cell Mol Gastroenterol Hepatol 2016;2:482–498; http://dx.doi.org/10.1016/j.jcmgh.2016.03.007)*

Keywords: Gut Microbiota; Innate Immunity; Germ-Free Mice; MyD88; Colitis; NGAL; Siderocalin; Neutrophils; IBD.

Inflammatory bowel disease (IBD) is the collective term for chronic idiopathic inflammatory diseases of the intestine, which are highly prevalent in North America and Europe.[1] The clinical symptoms of IBD may appear similar, however, its etiology and pathology may vary between IBD patients because genetics, diet, and environmental factors substantially influence the disease. Among environmental factors, gut microbiotal dysbiosis has been associated strongly with human IBD,[2] underscoring the involvement of host–microbe interactions.[3] Furthermore, IBD is associated with increased levels of a number of acute phase proteins (APPs) that drive or dampen the inflammatory response.[4] One such APP is lipocalin 2 (Lcn2, human ortholog, neutrophil gelatinase-associated lipocalin [NGAL]; also known as siderocalin, 24p3), a multifaceted

*Authors share co-first authorship.

Abbreviations used in this paper: **APP, acute phase protein; CD45, cluster of differentiation 45; cDNA, complementary DNA; CoH, co-housed; DMEM, Dulbecco's modified Eagle medium; DSS, dextran sulfate sodium; ELISA, enzyme-linked immunosorbent assay; FACS, fluorescence-activated cell sorter; FBS, fetal bovine serum; FITC, fluorescein isothiocyanate; GF, germ free; IBD, inflammatory bowel disease; IEC, intestinal epithelial cell; IL, interleukin; IL10R, interleukin-10 receptor; Lcn2, lipocalin 2; Lcn2KO, lipocalin 2 deficient; LPS, lipopolysaccharide; mAb, monoclonal antibody; MPO, myeloperoxidase; MyD88, myeloid differentiation primary response gene 88; NGAL, neutrophil gelatinase-associated lipocalin; PBS, phosphate-buffered saline; PCR, polymerase chain reaction; Rag1, recombination-activating gene 1; RBC, red blood cell; rRNA, ribosomal RNA; TLR, Toll-like receptor; TNF, tumor necrosis factor; WT, wild type.**

Most current article

2352-345X
http://dx.doi.org/10.1016/j.jcmgh.2016.03.007

antimicrobial innate immune protein whose expression is increased markedly in inflammatory diseases in both mice and human beings.[5–7] Accordingly, we have shown that fecal Lcn2 is a sensitive, broadly dynamic, noninvasive biomarker of intestinal inflammation.[8] However, several studies have shown that Lcn2 is not a mere bystander, but actively involved in several physiological and pathophysiological functions in IBD, renal diseases,[9–11] and cancer.[12,13]

Among its diverse functions, one well-established role of Lcn2 is to inhibit bacterial proliferation by chelating bacterial siderophores such as enterobactin, thus limiting iron acquisition.[14] However, Lcn2 alone cannot bind to ferric (Fe^{+3}) iron; instead, it requires the aid of small chemical molecules such as mammalian siderophore 2,5 dihyoxybenzoic acid or catechol to bind and transport iron in and outside of the cell.[15–17] A recent report showed that Lcn2 also can complex with Fe^{+3}-bound epigallocatechin gallate, a polyphenol from green tea.[16] Aside from its role in iron homeostasis, Lcn2 also is involved in establishing systemic hypoferremia during inflammation,[13,18] inducing epithelial cell secretion of chemokine interleukin (IL)8,[19,20] mediating tolerance to cellular iron overload,[21] and, furthermore, serves as a survival factor for epithelial cells.[22] Previously, we and Flo et al[23] have shown that Lcn2-knockout (*Lcn2*KO) mice are highly susceptible to lipopolysaccharide (LPS)- and bacterial-induced sepsis, respectively.[18] More recently, Allred et al[24] showed that Lcn2 limits the deleterious health effects induced by synthetic radionuclides by mediating their physiological transport via secondary ligand-based sequestration mechanisms. Altogether, these findings indicate broad and distinct physiological functions of Lcn2.

Neutrophils, the first responder cell type to most inflammation-inducing injuries, constitutively express and store Lcn2 within their specific granules. Lcn2 is indispensible for neutrophil infiltration, adhesion, and function.[25,26] Recently, we showed that Lcn2 preserves the bactericidal activity of neutrophil-derived host immune protein myeloperoxidase (MPO) by preventing its inactivation by bacterial siderophore enterobactin.[27] Lcn2 also is known to deactivate and modulate polarization of macrophages,[28] which are one of the most abundant leukocytes in the intestinal mucosa. In addition, Lcn2 facilitates mucosal regeneration[25,26] by promoting cell migration[29] and by forming heterodimers with matrix metalloproteinase-9, a metalloproteinase involved in tissue repair.[30] Although it is known that Lcn2 levels increased by several log orders of magnitude in various models of inflammation,[11,23] including murine colitis[7,8,31] and human IBD,[6,32,33] the role of Lcn2 in such inflammatory states is not known.

We hypothesized that Lcn2, which regulates gut bacterial growth, systemic inflammation, and mucosal repair, may play a key role in the gut homeostasis and IBD pathogenesis. Herein, we studied the basic mechanisms that regulate Lcn2 expression and, moreover, its role in intestinal pathobiology. We report that Lcn2 expression is regulated by microbiota-induced MyD88 signaling, which allows for rapid robust induction of this protein upon a range of challenges. Such Lcn2 expression helps keep microbiota in check, and consequently protects the intestine against colitis in multiple murine models.

Materials and Methods

Reagents and Antibodies

Reagent grade dextran sulfate sodium salt (DSS) (reagent grade; molecular weight, 36–50 kilodaltons; catalog number 160110) was purchased from MP Biomedicals (Solon, OH). Duoset enzyme-linked immunosorbent assay (ELISA) kits for mouse and human Lcn2 and keratinocyte-derived chemokine were obtained from R&D Systems (Minneapolis, MN). α-Hu-Lcn2 SYBR Green mix and the qScript complementary DNA (cDNA) synthesis kit were procured from Quanta BioSciences (Gaithersburg, MD). Guaiacol (2-methoxyphenol) was obtained from Alfa Aesar (Ward Hill, MA). MPO was procured from Sigma (St. Louis, MO). Ly6G antibody was purchased from Abcam (Cambridge, MA). Rat anti-mouse IL10 receptor (IgG_1) monoclonal antibody (αIL10R) and isotype control antibody (rat anti-mouse IgG1) were procured from BioXcell (West Lebanon, NH). Anti-mouse cluster of differentiation 45 (CD45)–Alexa Fluor 594 and CD326 monoclonal antibodies were procured from BioLegend (San Diego, CA). RegIIIγ and Ang4 antibodies were a kind gift from Dr Lora Hooper (UT Southwestern Medical Center, Dallas, TX). All other fine chemicals used in the present study were reagent grade and procured from Sigma.

Mice

*Lcn2*KO mice were originally generated by Dr Shizuo Akira (Department of Host Defense, Research Institute for Microbial Diseases, Osaka University, Japan.) on a C57BL/6 background and were obtained via Dr Kelly Smith (University of Washington, Seattle, WA). The offspring were cross-bred to obtain 4 possible genetic variants in the litter. Wild-type (WT) littermates of the respective gene (ie, *Lcn2*, *Il10*, myeloid differentiation primary response gene 88 [*Myd88*], or Toll-like receptor 5 [*Tlr5*]) KOs were used as controls throughout the study. All mice used in the present study were bred and maintained in specific pathogen–free conditions at Emory University and Georgia State University (Atlanta, GA), and The Pennsylvania State University (State College, PA). The institutional animal ethical committees at Emory University, Georgia State University, and The Pennsylvania State University approved the animal experiments.

Intestinal Epithelial Cell Culture

HT-29 human intestinal epithelial cells were cultured on 24-well plates in Dulbecco's modified Eagle medium (DMEM) supplemented with 10% fetal bovine serum (FBS) and 1% penicillin and streptomycin.[34] The epithelial cells were cultured on collagen-coated filters and then the polarized epithelial cells were stimulated with flagellin basolaterally in serum-free media. After 24 hours, basolateral and apical supernatants were collected separately and assayed for NGAL secretion via ELISA.

Immunoblotting

Neutrophils, obtained from 4 different individuals, were lysed in 0.5 mL RIPA buffer (Cell Signaling Technology, Inc,

Danvers, MA) with a protease inhibitor cocktail (Roche Diagnostics, Indianapolis, IN). The level of antimicrobial peptides RegIIIγ and Ang4 was analyzed in supernatant obtained from ileal explant culture as described by Singh et al.[35] Samples (25 μg/well) were fractionated by 12% sodium dodecyl sulfate–polyacrylamide gel electrophoresis and transferred to a polyvinylidene difluoride membrane and blocked for 1 hour in 5.0% nonfat milk at room temperature. The blots were incubated overnight at 4°C with α-Hu-Lcn2 or rabbit anti-mouse RegIIIγ or Ang4. After 3 washes, blots were incubated with anti-rabbit horseradish peroxidase and developed by a chemiluminescence reagent. β-actin was used as a loading control. Protein was quantified by a Bio-Rad (Bio-Rad Laboratories Inc, Hercules, CA) reagent.

T-Cell Transfer Colitis

Spleens harvested from female WT and *Lcn2*KO mice were crushed using frosted glass slides and washed with fluorescence-activated cell sorter (FACS) buffer (1× phosphate-buffered saline [PBS] with 2% FBS). After pelleting the cells, red blood cells (RBCs) were removed using RBC lysis buffer (Sigma) according to the manufacturer's protocol. Subsequently, the cells were resuspended in 2 mL FACS buffer, filtered through a 70-μm nylon cell strainer, and incubated with Phycoerythrin (PE)-conjugated rat anti-mouse CD4 and BB515-conjugated rat anti-mouse CD25 (BD Biosciences, San Diego, CA). $CD4^+CD25^-$ cells were sorted to more than 99.5% purity using a BD FACSAria III cell sorter. These cells were transferred (0.5×10^6 cells/mouse) to 4-week-old female recombination-activating gene 1 (*Rag1*) KO mice via tail vein injection and colitis was monitored after 8 weeks of $CD4^+CD25^-$ cell administration.

DSS-Induced Colitis

Eight-week-old male WT and *Lcn2*KO mice ($n = 4–5$) were administered 1.8% DSS (MP Biomedicals, Solon, OH) in drinking water over a period of 7 days.[36] This DSS concentration (1.8%) was ascertained after titrating it in WT mice. In brief, a set of WT mice from our colony were administered 1.5% or 2% DSS orally in drinking water and subsequently monitored for slow and steady induction of acute colitis over a period of 7 days. Lower doses of DSS (1.5%) were used in *Myd88*KO mice because these mice are highly susceptible to colitis.[37] Induction of colonic inflammation was confirmed via fecal occult blood, diarrhea, and loss of body weight. On day 7, mice were euthanized by CO_2 asphyxiation. Blood samples were collected at the time of euthanasia in a BD microtainer (Becton Dickinson, Franklin Lakes, NJ) via retro-orbital plexus. Hemolysis-free serum samples were obtained after centrifugation and stored at -80°C until further use.

Gut epithelial barrier function was evaluated in DSS-treated WT and *Lcn2*KO mice using fluorescein isothiocyanate (FITC)-dextran (4 kilodaltons; Sigma). Mice were gavaged orally with FITC-dextran (50 mg/100 g body weight) as a permeability tracer. After 6 hours, serum was collected and FITC-dextran was analyzed using fluorescence spectroscopy.

IL10R Neutralization-Induced Chronic Colitis

Colitis was induced in *Lcn2*KO mice and their WT littermates by administering IL10R (IgG1) monoclonal antibody (α-IL10R mAb) as described earlier.[38,39] In brief, 5-week-old male WT and *Lcn2*KO mice were administered weekly anti-mouse α-IL10R mAb (1.0 mg/mouse, intraperitoneally) for up to 4 weeks. Body weight was measured every week before injection. One week after the last injection the mice were euthanized and analyzed for standard colitic parameters. In some experiments, 4-week-old male *Lcn2*KO mice were maintained on ampicillin (1.0 g/L) and neomycin (0.5 g/L)[40] in drinking water for 4 weeks and received α-IL10R mAb weekly as described earlier. Control mice were given isotype control (rat anti-mouse IgG_1) antibody.

Co-housing

Immediately after weaning (3 weeks old), male *Lcn2*KO and their WT littermates were co-housed with male *Il10*KO mice at a ratio of 2:3 (WT or *Lcn2*KO:*Il10*KO) in each cage, for up to 8 weeks. Animals were monitored regularly for body weight and signs of colonic inflammation including sticky stool, occult blood, and rectal prolapse. The data provided the total number of *Il10*KO mice, which developed rectal prolapse within 8 weeks after co-housing with either WT or *Lcn2*KO mice.

Bone Marrow Chimera Generation

Eight-week-old *Lcn2*KO and their WT littermates were exposed to whole-body radiation (850 rads) using a Shepherd Cesium Irradiator (JL Shepherd and Associates, San Fernando, CA), and allowed them to stabilize for 2 hours. Femurs from 4-week-old female WT and *Lcn2*KO donor mice were flushed with DMEM supplemented with 10% FBS. Subsequently, the bone marrow cells were suspended in the RBC lysis buffer and incubated for 5 minutes to lyse erythrocytes. After incubation, cells were immediately pelleted by centrifugation at 400 × g for 5 minutes and resuspended in DMEM media supplemented with FBS (10%). Before injection, the cells were washed and suspended in sterile Hank's balanced salt solution. After a stabilization period, bone marrow cells (10^7 cells/mouse) in Hank's balanced salt solution were administered to irradiated mice via retro-orbital injection to generate WT→*Lcn2*KO and *Lcn2*KO→WT bone marrow chimera. We also generated WT→WT and *Lcn2*KO→*Lcn2*KO bone marrow chimera to use as a control in the present study. Subsequently, mice were switched immediately to drinking water containing neomycin (2 mg/mL) for the initial 2 weeks and then allowed 6 more weeks for reconstitution. This process generated approximately 95%–99% chimerism as described earlier.[41,42]

MPO Activity

Colonic tissues from WT and *Lcn2*KO mice on different treatments were homogenized in 0.5% hexadecyltrimethylammonium bromide (Sigma) in potassium phosphate buffer (pH 6.0). Subsequently, the mixture was

freeze–thawed 3 times and sonicated and centrifuged at 14,000 × g for 10 minutes at 4°C. Clear supernatants were collected and MPO assay was performed using the guaiacol method as described by Singh et al.[27] Briefly, the suitably diluted supernatants in potassium phosphate buffer were dispensed in 96-well plates (Corning, Corning, NY) in triplicate. The reaction was initiated by adding final concentrations of 100 mmol/L guaiacol and 6.7 × 10^{-3}% H_2O_2. The change in absorbance at 470 nm was measured over a period of 10 minutes at 30-second intervals. One unit of MPO activity was defined as the amount that increased absorbance at 470 nm by an outside diameter of 1.0 per minute at 25°C, calculated from the initial rate of reaction using guaiacol as the substrate.

Total Bacterial Load Quantification

Total bacterial DNA was isolated from equal amounts of feces (50 mg) using the QIAamp DNA Stool Mini Kit (Qiagen Inc, Valencia, CA). After 1/10 dilution, DNA was subjected to quantitative polymerase chain reaction (PCR) using the Quanti Fast SYBR Green PCR kit (Bio-Rad) with universal 16S ribosomal RNA (rRNA) primers 8F: 5'-AGAGTTTGATCCTGGCTCAG-3', and 338R: 5'-CTGCTGCCTCCCGTAGGAGT-3' to measure total bacteria. Fecal bacterial load is expressed as the fold change relative to their WT littermates using a standard curve generated with *Escherichia coli* DNA. The level of *EntA*-expressing gut bacteria was analyzed by the following primers: *EntA*-F: GGGCTGGAACTGGCGGGTAG, and *EntA*-R: CTGGCGAGGTCAGAGGCGAG.

Quantitative Reverse-Transcription PCR

Total RNA was isolated from colonic tissue using TRI reagent (Sigma) per the manufacturer's protocol. The cDNA was synthesized from 1.0 μg of purified RNA using the qScript cDNA Synthesis Kit (Quanta BioSciences). Real-time PCR was performed using the Step One Plus Real-Time PCR System (Applied Biosystems Foster City, CA) in a 25-μL reaction mixture containing cDNA, SYBR Green Master Mix (Quanta BioSciences), and mouse-specific oligonucleotides (*Lcn2*-F: AAGGCAGCTTTACGATGTACAGC, *Lcn2*-R: CTTGCACATTGTAGCTGTGTACC; *36B4*-F: TCCAGGCTTTGGGCATCA, *36B4*-R: CTTTATTCAGCTGCACATCACTCAGA) as mentioned earlier.[43] The primers were procured from The Huck Institutes of the Life Sciences, Genomic Core Facility, and The Pennsylvania State University. The relative fold-difference between different groups was calculated using the comparative Ct [$2^{-\text{delta delta Ct}}$ ($2^{-\Delta\Delta\ Ct}$)] method. The *36B4* gene was used as an internal standard to calculate the relative expression.

ELISA

Fecal samples were prepared as described previously.[8] In brief, frozen or freshly collected feces were dissolved to make a 100 mg/mL fecal suspension in PBS containing 0.1% Tween 20 and vortexed for 30 minutes at room temperature. Samples then were centrifuged at 4°C for 10,000 × g for 10 minutes to collect clear supernatants. Blood was collected at the time of mice euthanasia in a BD microtainer (Becton Dickinson) via retro-orbital plexus. To measure colonic tumor necrosis factor (TNF)α, colonic tissue was homogenized in RIPA buffer and the clear supernatant was used to measure TNFα. Hemolysis-free sera was obtained after centrifugation and stored at -80°C until further use. Mouse Lcn2 and TNFα Duoset ELISA kit (R&D Systems) were used to quantify serum and fecal Lcn2 and colonic TNFα per the manufacturer's protocol. Likewise, serum amyloid A was quantified in serum using an ELISA kit. Serum immunoreactivity to LPS and flagellin was analyzed as described earlier.[44]

Histology and Immunohistochemistry

After euthanasia, Swiss rolls of colons were fixed overnight in 10% neutral buffered formalin solution and then stored in 70% ethanol. Colons were processed for paraffin embedding and serial sections (5 μm) were collected and stained with H&E. Histologic scoring was performed as described previously.[45]

For neutrophil staining, the paraffin-embedded colon sections were stained with rat anti-mouse antibody specific to neutrophil marker Ly6G (Abcam) and visualized under fluorescent microscopy. An appropriate negative isotype control (rat IgG2b; Abcam) was included to omit nonspecific staining.

Immunofluorescence staining was performed in paraffin-embedded colon sections from control and DSS-treated WT mice using anti-mouse antibodies specific to Lcn2, CD45 (leukocyte marker), and CD326 (epithelial cell adhesion molecule, a marker for epithelial cells). In brief, deparaffinized and rehydrated colon sections initially were blocked with normal horse serum (5% in PBS) and then incubated with primary antibodies (Lcn2 [R&D Systems] and CD45–Alexa Fluor 594 [BioLegend], or Lcn2 and CD326–Alexa Fluor 594 [BioLegend]) for 18 hours in the dark at 4°C. After washing, sections were incubated with secondary antibody against Lcn2 (rabbit anti-goat Alexa Fluor 488; Molecular Probes, Inc, Eugene, OR) for 1 hour at room temperature. Sections finally were washed with PBS and mounted with Fluoroshield with 4′,6-diamidino-2-phenylindole (Sigma, St. Louis, MO). Images were acquired using a Keyence BZ-9000 fluorescence microscope (Keyence Corporation of America, Itasca, IL).

16S rRNA Gene Pyrosequencing

Sample collection and DNA isolation. Fecal pellets from age- and sex-matched *Lcn2*KO (n = 4) and WT (n = 5) littermates were collected under hygienic conditions and stored in sterile vials at -20°C before processing. DNA was extracted from 0.5 g fecal material using the MO-BIO PowerSoil DNA isolation kit (MO-BIO Laboratories, Carlsbad, CA) according to the manufacturer's instructions. The DNA concentration was analyzed using the Qubit 2.0 Fluorometer and related high-sensitivity double-stranded DNA kit, according to the manufacturer's instructions (Life Technologies, Grand Island, NY). DNA concentrations were standardized to 10 ng/μL to be used in library preparation.

Illumina tag PCR. DNA isolates were subject to duplicate 25 uL Illumina tag PCRs (Illumina, San Diego, CA) to amplify the V4 region of the 16S rRNA gene using primers 515F and 806R as detailed in Earth Microbiome Project (http://www.earthmicrobiome.org/). Each reaction contained final concentrations of 1 × PCR buffer, 0.8 umol/L deoxynucleotides (dnTPs), 4 umol/L 515F Illumina barcoded forward primers, 4 umol/L 806R reverse primers, 0.25 U Taq polymerase, and 10 ng of template DNA. PCR was performed using the PTC-200 Thermocycler (MJ Research Incorporation, Waltham, MA). Reactions were held at 94°C for 3 minutes to allow for the DNA to denature, followed by 35 cycles at 94°C for 45 seconds, 50°C for 60 seconds, and 72°C for 90 seconds, with a final extension time of 10 minutes at 72°C followed by holding at 4°C. PCR products were visualized on a 2% agarose E-gel (Life Technologies, Carlsbad, CA).

Library preparation and sequencing. The DNA concentration of successful PCR products was analyzed using the Qubit 2.0 Fluorometer, and equimolar amounts of each PCR product were pooled and Solid-phase reversible immobilization (SPRI)-bead purified using the Agencourt AMPure XP-PCR Purification Kit according to the manufacturer's instructions (Beckman Coulter, Indianapolis, IN). Cleaned, pooled libraries were quality checked using the Agilent 2100 Bioanalyzer and the related Agilent High-Sensitivity DNA Chip, according to the manufacturer's instructions (Agilent Technologies, Santa Clara, CA).

University of Tennessee-Knoxville (Knoxville, TN) performed the sequencing. Library pools were size-verified using the Fragment Analyzer CE (Advanced Analytical Technologies, Inc, Ames, IA) and quantified using the Qubit high-sensitivity double-stranded DNA kit (Life Technologies, Carlsbad, CA). After dilution to a final concentration of 1 nmol/L containing 10% PhiX V3 library control (Illumina, San Diego CA), the library pools were denatured for 5 minutes in an equal volume of 0.1 N NaOH, further diluted to 12 pmol/L in HT1 buffer (Illumina), and sequenced using the IlluminaMiSeq V2 300 cycle kit cassette and set for 2 × 150 base (paired-end reads).

Sequences analysis. Forward and reverse reads were paired, trimmed at a length of 252 bp, and quality filtered with an expected error of less than 1% using USEARCH v7.[46] Operational taxonomic units were picked using the open reference USEARCH61 algorithm,[46] and taxonomy assignment was performed using the Greengenes 16S rRNA gene database (13-8 release; 97%). Sequences that did not match the database subsequently were clustered using de novo clustering.[46]

Beta diversity. Beta diversity was estimated by calculation of unweighted UniFrac distances between samples. Principal coordinate analysis was performed on the UniFrac distance matrices. The analysis of similarities (ANOSIM) metric was used to determine the degree to which metadata parameters explained patterns in the UniFrac distance matrix.

Microarray Analysis

Microarray analyses were performed in biological triplicates using colonic tissue of 8-week-old male *Lcn2*KO mice and their WT littermates at the Emory Biomarker Microarray Core. Briefly, messenger RNA samples were reverse-transcribed, amplified, labeled, and used to probe mouseWG-6 v2 chips purchased from Affymetrix (Santa Clara, CA). Samples were assayed using a Molecular Devices Gene Pix (4100A) (Silicon Valley, CA), and raw fluorescence readings were processed by an algorithm designed to reduce spurious readouts of gene activation. Microarray data were quantile-normalized using freely available scripts written in R (www.R-project.org). Significantly altered genes were identified using significance of analysis of microarray analyses and assessed by hierarchal clustering and principle component analysis using Spotfire Decision Site for Functional Genomics software (TIBCO, Somerville, MA) to determine relatedness of gene expression patterns resulting from loss of Lcn2.

Statistical Analysis

Data are presented as means ± SEM. Significance of difference between 2 groups was analyzed by an unpaired *t* test. One-way analysis of variance followed by the Dunnett (when the mean of each column was compared with the mean of a control column) or the Tukey (when the mean of each column was compared with the mean of every other column) multiple comparison test was used to compare more than 2 groups. All statistical analyses were performed using GraphPad Prism 6.0 program (GraphPad Software, Inc, La Jolla, CA).

Results

Inflammatory Conditions and Microbial Products Up-Regulate Lcn2 Expression In Vivo and In Vitro

IBD is associated with increased levels of fecal and serum Lcn2. Although many cell types have the capacity to make Lcn2 in vitro, it is not clear, in vivo, which cell types produce Lcn2 basally and upon colitis. Herein, we examined the colonic expression of Lcn2 in DSS-induced colitic WT mice and spontaneously colitic *Il10*KO and *Tlr5*KO mice in comparison with noncolitic controls. As shown in Figure 1*A*, the expression of Lcn2 is not confined to the gut epithelia but also includes other cell types in the colon. This observation was confirmed further by examining the colocalization of Lcn2 with leukocytes and/or epithelial cells in the colonic tissue sections of DSS-treated mice using dual immunofluorescence staining (Supplementary Figure 1*A*). To further dissect the relative contribution of immune and nonimmune cells to the pool of systemic Lcn2, we generated Lcn2 bone marrow chimeras and measured their Lcn2 expression. Our results showed that nonimmune cells are the major contributor of circulating Lcn2 at the basal level as well as in response to DSS and LPS challenge in vivo (Supplementary Figure 2). In comparison, immune cells also contribute to the pool of circulating Lcn2, but to a substantially lesser extent.

A previous study reported that the intestinal epithelial cells could be one of the major producers of Lcn2 during IBD.[47] Consistent with that study, we also found that HT29 cells (human intestinal epithelial cell line) spontaneously secrete Hu-Lcn2 (also known as NGAL), and its secretion

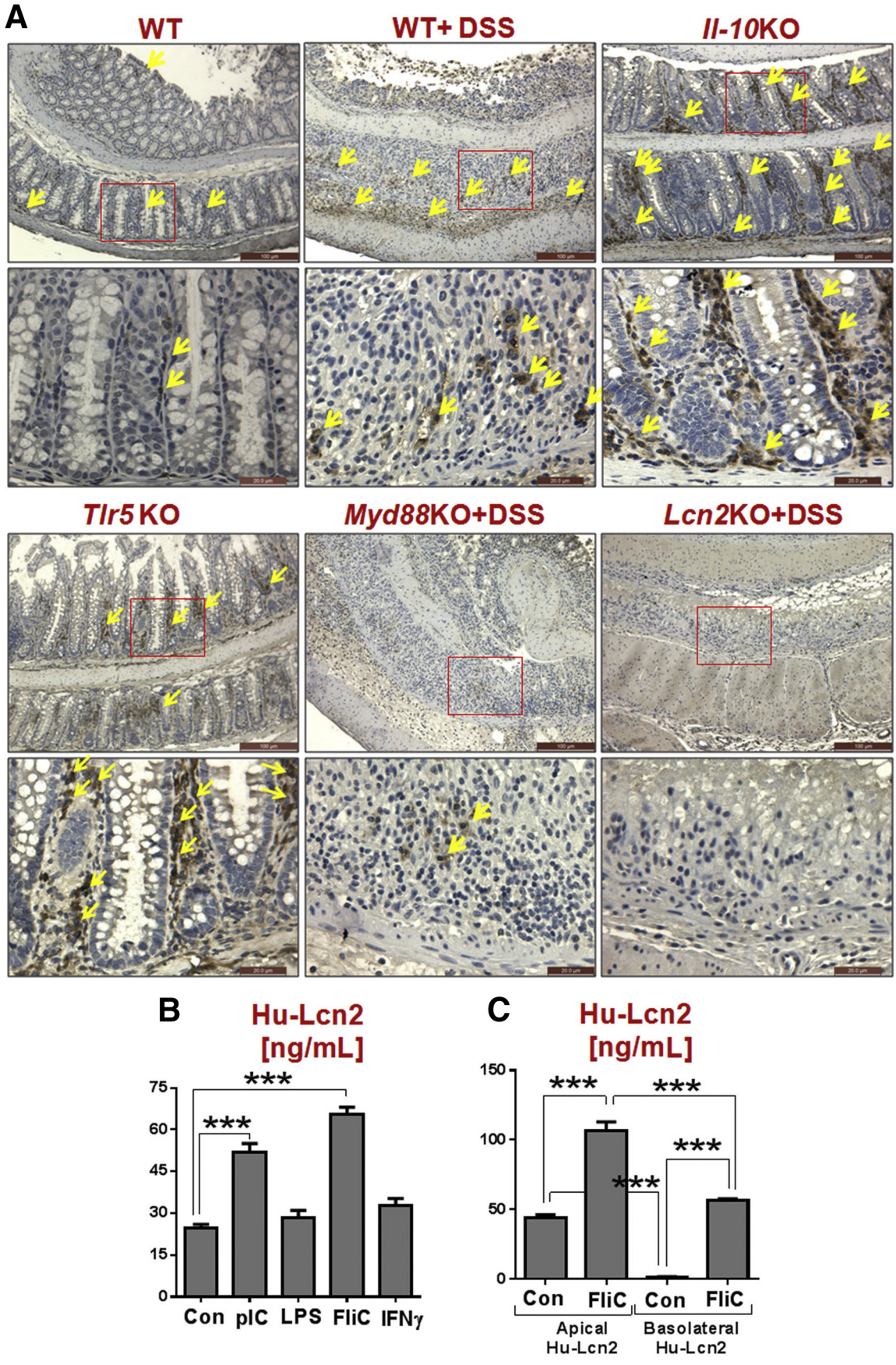
A
WT
WT+ DSS
Il-10KO
Tlr5 KO
Myd88KO+DSS
Lcn2KO+DSS
B
Hu-Lcn2
[ng/mL]
75
60
45
30
15
0
***
***
Con
pIC
LPS
FliC
IFNγ
C
Hu-Lcn2
[ng/mL]
150
100
50
0
***
***
***
***
Con
FliC
Con
FliC
Apical
Hu-Lcn2
Basolateral
Hu-Lcn2

was augmented further upon stimulation with synthetic double-stranded RNA [polyinosinic acid:cytidylic acid (poly I:C)] and flagellin (Figure 1*B*), which are TLR3 and TLR5 ligands, respectively. However, HT29 cells failed to induce Hu-Lcn2 in response to either LPS or interferon-γ (Figure 1*B*). To assess the vectorial direction of Hu-Lcn2 secretion, we measured Hu-Lcn2 secretion in polarized HT29 cells and found that most of the spontaneous Hu-Lcn2 secretion was confined to the apical compartment with negligible amounts in the basolateral side when unstimulated (Figure 1*C*). Surprisingly, HT29 cells stimulated with basolateral flagellin increased their Hu-Lcn2 secretion in the apical compartment by only 2-fold, whereas the basolateral secretion of Hu-Lcn2 was increased by approximately 30-fold (Figure 1*C*).

We also found that human neutrophils remain a rich source of intracellular Hu-Lcn2 because they expressed approximately 6-fold more Hu-Lcn2 than HT29 epithelial cells. Interestingly, even though human neutrophils contained both the monomeric and dimeric forms of Lcn2 in the intracellular pool,[48] neutrophils only secreted the dimeric form of Lcn2 upon stimulation with a variety of stimuli (Supplementary Figure 3). In comparison, nonimmune cells such as intestinal epithelial cells (IECs) produce and secrete only the monomeric form of Hu-Lcn2.[48] Altogether, these results suggest that differential secretion patterns of Hu-Lcn2 by neutrophils and the IECs contribute to the intracellular and extracellular/systemic pool of Hu-Lcn2 during normal and inflamed states.

Gut Microbiota Regulates Lcn2 Expression in a MyD88-Dependent Manner

Among its diverse functions, Lcn2 exerts bacteriostatic effects by chelating bacterial siderophore and inhibiting bacterial proliferation.[14,23] To examine whether the gut microbiota influences Lcn2 expression, we measured basal Lcn2 levels in germ-free (GF) and conventional WT mice. GF mice showed significantly reduced serum and fecal Lcn2 (Figure 2*A*). Upon conventionalization of GF mice via oral gavage of cecal contents from conventional WT mice, the colonic and ileal messenger RNA transcripts of *Lcn2* were increased at day 4 and peaked at day 7 (Figure 2*B*). Similarly, a time-dependent increase in fecal Lcn2 was observed, which peaked at day 4 in conventionalized GF mice (Figure 2*C*). These results suggest that the gut microbiota is required to maintain normal levels of Lcn2 in the lumen and circulation, which may in turn regulate the microbiota, specifically by chelating the iron-scavenging siderophores.

Next, we asked whether the innate and adaptive arms of the immune system are involved in regulating Lcn2 expression during intestinal inflammation. *Myd88*KO mice, which lack all TLR signaling except TLR3, showed low levels of systemic and colonic Lcn2 in comparison with their WT littermates (Figure 2*D*). Interestingly, *Myd88*KO mice failed to up-regulate either fecal or serum Lcn2 to the extent of WT mice in response to DSS treatment (Figure 2*E* and *F*), even though these mice developed severe pathology (data not shown) similar to that observed earlier.[37,49] In contrast, the colonic and systemic Lcn2 were unaltered in adaptive immune response–deficient *Rag1*KO mice (data not shown). Altogether, these data suggest that Lcn2 is a bacterially induced and in part MyD88-regulated protein. In addition, the association between increased susceptibility to DSS-induced colitis and the impaired Lcn2 response in *Myd88KO* mice suggest that Lcn2 may have a protective role against gut inflammation.

Lcn2-Deficient Mice Display Altered Colonic Gene Expression and Gut Bacterial Dysbiosis

To study the effects of Lcn2 deficiency on gut physiology, we performed a microarray analysis to examine global colonic gene expression in *Lcn2*KO mice relative to age- and sex-matched WT littermates in biological triplicates. Loss of *Lcn2* resulted in significant up-regulation of 46 genes and down-regulation of 92 other genes in the colons of *Lcn2*KO mice assayed (Supplementary Figure 4). These changes are consistent with the notion that to compensate for Lcn2 deficiency, *Lcn2*KO mice have significantly up-regulated acute phase protein (α-1-antitrypsin [serpin peptidase inhibitor, clade A (α-1 antiproteinase, antitrypsin), member 1b]), major urinary proteins, which are members of the lipocalin superfamily, and cation transporters (*Slc25a36* and *Slco1b2*) in the colon. Notably, *Fetuin-A* and *vitronectin*, which favor bacterial adherence, were up-regulated significantly in the colons of *Lcn2*KO mice.[50,51] Accordingly, *Lcn2*KO mice showed 3-fold more bacteria in feces, most of which express *entA* (2,3-dihydro-2,3-dihydroxybenzoate dehydrogenase, an enzyme involved in enterobactin synthesis) (Figure 3*A*). *Lcn2*KO mice harbor a large proportion of gram-negative bacteria (eg, *Enterobacteriaceae*) in the gut, as monitored by using Drigalski lactose agar medium (Figure 3*B*). Concomitantly, increased fecal flagellin, which

Figure 1. (***See previous page***). **Increased colonic Lcn2 in various murine models of colitis.** Age-matched male BL6 WT, *Il10*KO, *Tlr5*KO, *Myd88*KO, and *Lcn2*KO mice (n = 4) were euthanized and Swiss rolls were made from the colon. WT mice were treated with DSS (1.8%) for 1 week. (*A*) Images show the immunostaining of Lcn2 (brown staining) in colons. *Lower panel* of each image show the high-magnification image (400×) of the *boxed* area in the respective *upper panels*. Yellow arrows denote Lcn2 immunostained cells in colonic tissue sections. HT29 cells were stimulated with the indicated stimuli with either Salmonella flagellin (high-performance liquid chromatography purified, 100 ng/mL) and Salmonella LPS (10 μg/mL), synthetic double-stranded RNA polyinosinic acid:cytidylic acid (poly I:C) (10 μg/mL), and proinflammatory cytokine interferon (IFN)γ (100 U/mL) in serum-free media for 24 hours. To study the vectorial direction of Lcn2-secretion polarized epithelial cell monolayer, HT29 cells were grown on 5-cm^2 filters. Flagellin (100 ng/mL) was applied basolaterally. (*B* and *C*) *Bar graphs* represent Hu-Lcn2 produced in the supernatant obtained from control and stimulated IECs. Results are expressed as means ± SEM. One-way analysis of variance with (*B*) the Dunnett test and (*C*) the Tukey multiple comparison test were used. $P < .05$ was considered statistically significant. ***$P < .001$. Con, control; FliC, flagellin; pIC, polyinosinic acid:cytidylic acid.

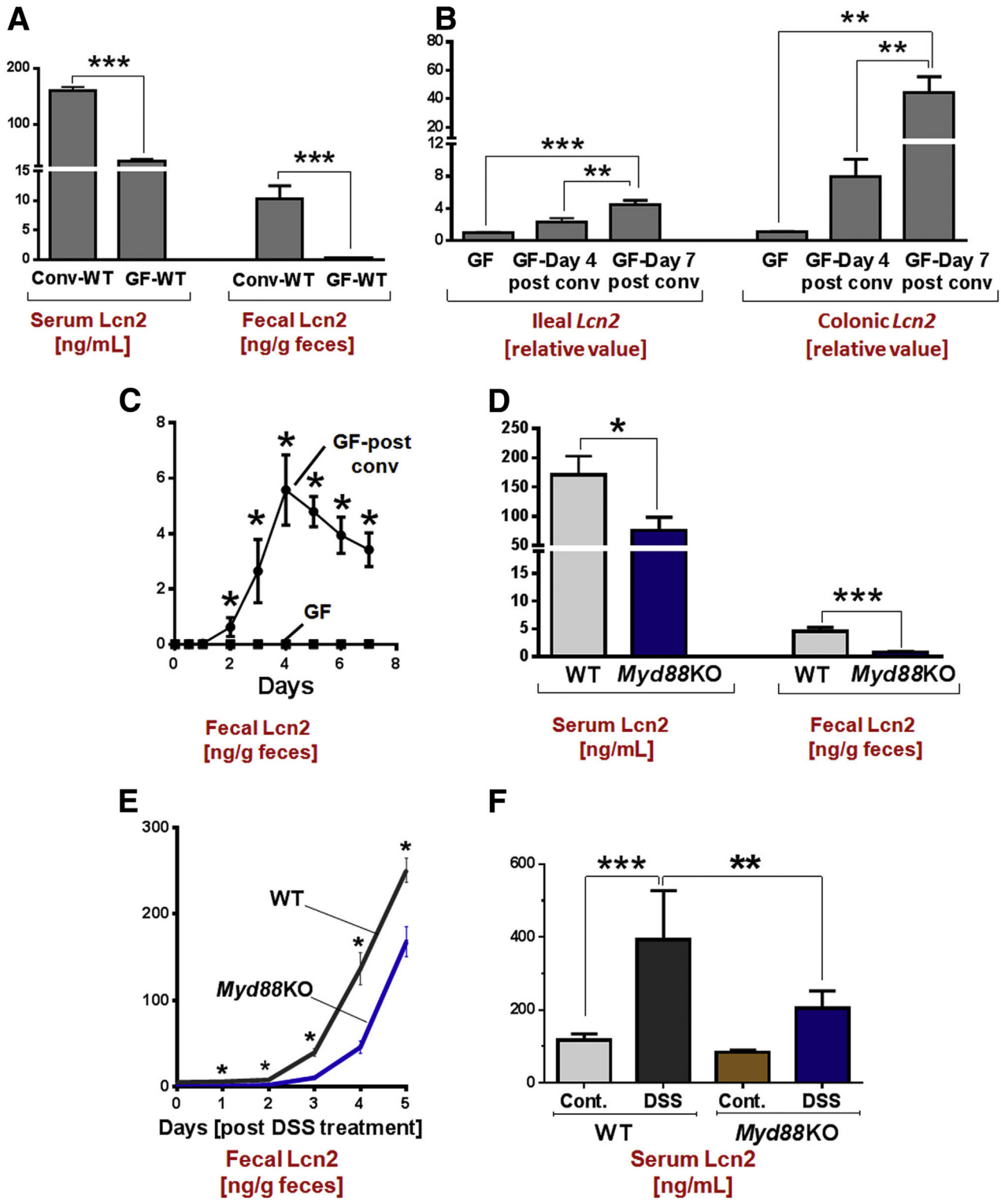

Figure 2. Reduced systemic and fecal Lcn2 in GF and MyD88-deficient mice. Lcn2 was measured in age- and sex-matched GF and conventional mice (n = 5-6) using ELISA. Messenger RNA transcript of ileal and colonic *Lcn2* was examined using quantitative reverse-transcription polymerase chain reaction. (*A*) Serum and fecal Lcn2 levels in conventionalized and GF mice. (*B*) mRNA transcript of *Lcn2* in ileum and colon. (*C*) Time-dependent excretion of fecal Lcn2 in GF and conventionalized GF mice. (*D*) Serum and fecal Lcn2 in *Myd88*KO mice and their WT littermates (n = 5). Colitis was induced by orally administering DSS (1.5%) to 8-week-old male WT and *Myd88*KO mice. (*E*) *Line graph* represents the time-dependent increase in fecal Lcn2 after DSS stimulation. (*F*) *Bar graph* represents serum Lcn2 control and DSS-treated WT and *Myd88*KO mice. Results are expressed as means ± SEM. (*A*, *C*, *D*, and *E*) Unpaired *t* test and (*B* and *F*) 1-way analysis of variance with the Tukey multiple comparison test were used. $P < .05$ was considered statistically significant. $^{*}P < .05$, $^{**}P < .01$, and $^{***}P < .001$. post conv, post conventionalization with WT gut microbiota.

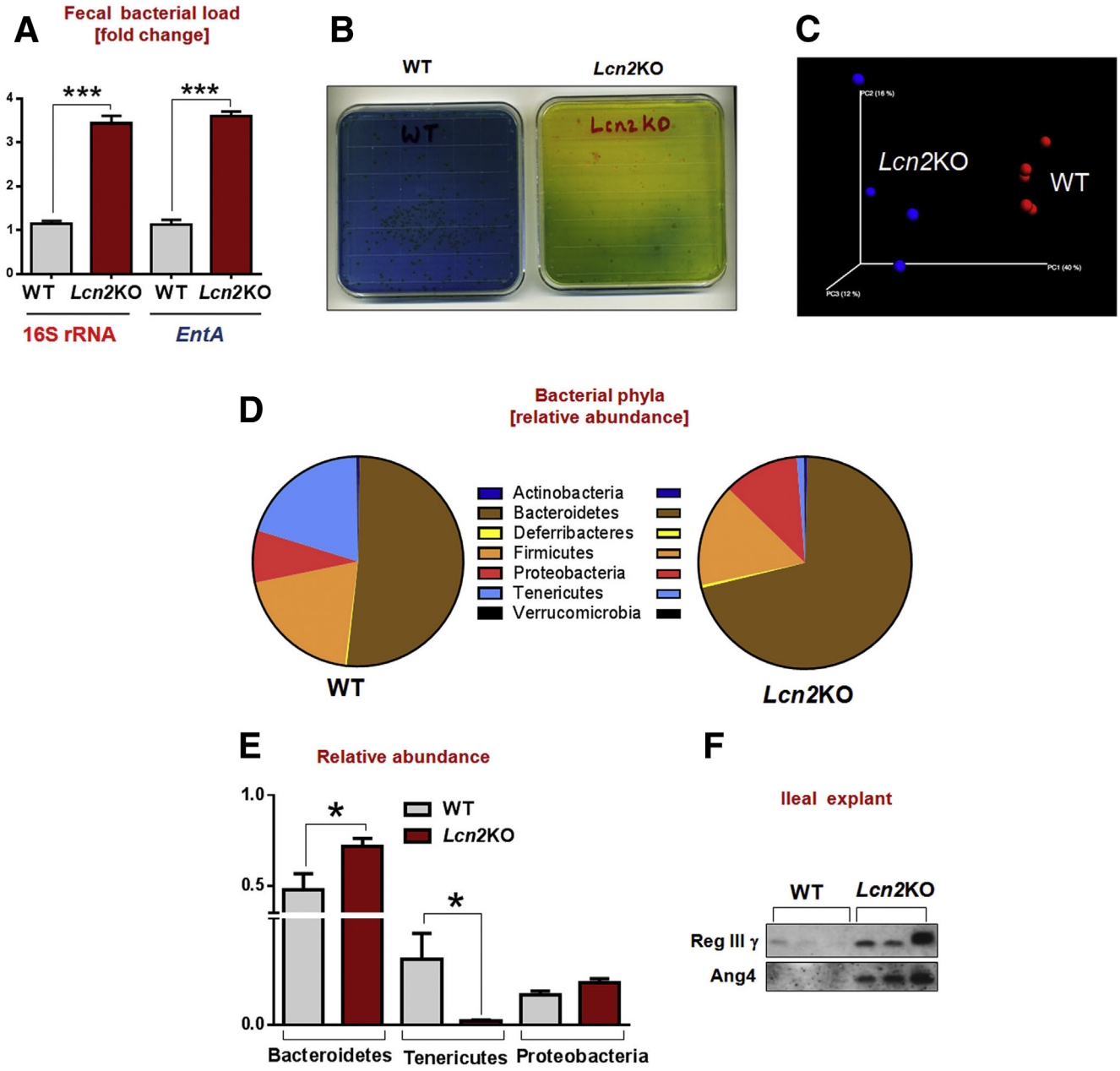

Figure 3. Increased gut bacterial load and distinct bacterial community in Lcn2-deficient mice. (*A*) Gut bacterial load analyzed by real-time polymerase chain reaction using universal primer of bacterial 16S rRNA and *entA* gene. (*B*) Gram-negative bacterial analysis by Drigalski lactose agar. (*C*) Principal coordinate analysis of unweighted UniFrac distances between fecal microbial communities from 12-week-old *Lcn2*KO and their WT littermates (n = 4-5). Each *point* represents a discrete sample. Samples clustered closely together have similar bacterial community structure but distant points have distinct communities. (*D* and *E*) Relative abundance of major bacterial phyla in *Lcn2*KO mice and their WT littermates. (*F*) Immunoblot of antimicrobial proteins Reg-IIIγ and Ang4 in the ex vivo ileal explants from WT and *Lcn2*KO mice. Results are expressed as means ± SEM. (*A* and *E*) An unpaired *t* test was used. $P < .05$ was considered statistically significant. $^{*}P < .05$ and $^{***}P < .001$.

might be derived predominantly from gram-negative bacteria flagella, was found in *Lcn2*KO mice (data not shown). Our present findings are reminiscent of the gut microbiotal dysbiosis of *Tlr5*KO mice, which are predisposed to the development of moderate to robust spontaneous colitis.[7] However, unlike *Tlr5*KO mice, *Lcn2*KO mice did not develop spontaneous gut inflammation (data not shown).

To further evaluate the dysbiotic microbiota in *Lcn2*KO mice, we subjected the mice fecal samples to 16S rRNA sequencing. Principal coordinate analysis of unweighted UniFrac distances between fecal microbial communities showed a distinct clustering by genotype, suggesting that bacterial communities are significantly different in *Lcn2*KO and WT mice (Figure 3*C*). Moreover, the uses of only a few

operational taxonomic units were sufficient to discriminate microbiota from each experimental group (Supplementary Figure 5). *Bacteroidetes* phylum, which is more prevalent in IBD,[52] was found increased in *Lcn2*KO mice (Figure 3*D* and *E*). Notably, *Tenericutes*, a bacterial phylum that decreases upon DSS challenge,[53] also was reduced in mice lacking Lcn2 (Figure 3*D* and *E*). To a lesser extent, the phylum *Proteobacteria*, which is regarded as opportunistic, colitogenic, and, a marker of dysbiosis, was increased modestly in *Lcn2*KO mice (Figure 3*D* and *E*). The gut bacterial dysbiosis and increased bacterial burden in *Lcn2*KO mice did not result in spontaneous gut inflammation but, rather, eventuated in increased expression of Paneth cell–specific antimicrobial proteins Ang4 and RegIII-γ[54] (Figure 3*F*), possibly to compensate for Lcn2 deficiency.

Lcn2-Deficient Mice Are Susceptible to DSS-Induced Acute Colitis and Display Colitogenic T Cells

Lcn2 prevents mucosal damage by promoting mucosal regeneration in an experimental model of gastric damage.[29] However, mice lacking lipocalin-type prostaglandin D synthase, a member of the lipocalin family of proteins, are protected from DSS-induced colitis.[55] However, it still is unclear whether Lcn2 show procolitogenic or anticolitogenic properties during IBD. To study whether deficiency of Lcn2 reduces or exacerbates murine colitis, 8-week-old *Lcn2*KO and their WT littermates were given 1.8% DSS in drinking water for 7 days. As shown in Supplementary Figure 6*A* and *B*, *Lcn2*KO mice showed greater body weight loss and colonic inflammation as characterized by more occult blood, colon shortening, and splenomegaly (Supplementary Figure 6*C*). In addition, the level of systemic inflammatory marker serum amyloid A and intestinal permeability, as measured by FITC-dextran, were increased in DSS-treated *Lcn2*KO mice when compared with WT littermates (data not shown). Interestingly, the increased DSS-induced pathology in *Lcn2*KO mice was not accompanied by increased levels of colonic MPO, a marker of neutrophil infiltration (Supplementary Figure 6*D*) despite the observed extensive colonic damage (Supplementary Figure 6*E* and *F*). In accordance, we performed immunofluorescence staining for neutrophil-specific marker Ly6G and reduced neutrophil infiltration was observed in the colonic sections obtained from *Lcn2KO* mice (Supplementary Figure 6*G* and *H*), which explains the impaired MPO activity in Lcn2-deficient mice. Such compromised neutrophil recruitment also may account for severe colitis development in *Lcn2*KO mice because neutrophils play a key role in mucosal healing by producing the mediators required for inflammation resolution and promoting the recruitment of other immune cells.[56]

Next, we asked whether Lcn2 deficiency also could impact the immune cell–mediated colitis. Accordingly, we used the adoptive T-cell transfer model of colitis to investigate the colitogenic potential of Lcn2-deficient T cells. Briefly, we transferred FACS-sorted $CD4^+CD25^-$ T cells from WT and *Lcn2*KO mice to *Rag1*KO mice and monitored induction of colitis. As shown in Figure 4, recipients of *Lcn2*KO effector T cells (*Lcn2*KO-R) showed exacerbated and robust colitis relative to mice receiving WT T cells. Such exacerbated colitis featured greater loss in body weight, colon shortening, colonic inflammation (Figure 4*A–C*), and increased infiltration of inflammatory cells as observed in H&E-stained colons (Figure 4*D* and *E*). Collectively, these findings suggest that Lcn2 deficiency not only may dysregulate gut microbiota homeostasis, but also could induce substantial intrinsic changes in immune cells (ie, neutrophils, T cells) that may contribute to the augmented colitis phenotype observed in *Lcn2*KO mice.

Lcn2KO Mice Are Prone to Chronic Colitis on IL10R Neutralization

The earlier-described results suggest that *Lcn2*KO mice might be particularly prone to develop inflammation upon induction of immune dysregulation. Hence, we used anti-IL10R monoclonal antibody (αIL10R) to neutralize IL10 signaling to delineate their colitis susceptibility. Previously, we showed that αIL10R treatment reproducibly induces a uniform (100%) robust colitis in *Tlr5*KO mice.[39,42] *Lcn2*KO mice and their WT littermates were subjected to weekly injections of αIL10R (intraperitoneally) for up to 4 weeks and then euthanized 1 week after the last (fourth) injection. αIL10R-treated *Lcn2*KO mice showed classic features of chronic colitis such as body weight loss, shrunken ceca, splenomegaly, and colomegaly (Figure 5*A–D*). Notably, 3 of 8 *Lcn2*KO mice developed rectal prolapse, a severe and irreversible form of colitis, after the fourth injection. Furthermore, enhanced immune cell infiltration was observed in the colons of αIL10R-treated *Lcn2*KO mice when compared with their αIL10R-treated WT littermates (Figure 5*E*). However, colonic MPO was not increased in αIL10R-treated *Lcn2*KO mice (data not shown), which possibly is owing to reduced neutrophil infiltration in *Lcn2*KO mice as observed in the DSS-induced acute colitis (Supplementary Figure 6*G* and *H*). In addition, αIL10R-treated mice showed increased systemic immunoreactivity toward bacterial products LPS and flagellin in both WT and *Lcn2*KO mice (Figure 5*F*). Notably, *Lcn2*KO mice showed more serum immunoreactivity to LPS than WT, suggesting that increased dissemination of microbial products in *Lcn2*KO mice might contribute further in augmenting systemic inflammation and thus colitis.

Exacerbated Colitis in Lcn2KO *Mice Is Microbiota Dependent*

Deficiency of Lcn2 leads to an increase in gut bacterial load and favors the expansion of *Bacteroidetes*, which are known to be associated with colitis in mice. Hence, we next asked to what extent gut bacterial dysbiosis in *Lcn2*KO mice contributes to their proneness to develop colitis on IL10R neutralization. *Lcn2*KO mice were pretreated with broad-spectrum antibiotics (ampicillin and neomycin in drinking water) for up to 1 week and then subjected to 4 weekly

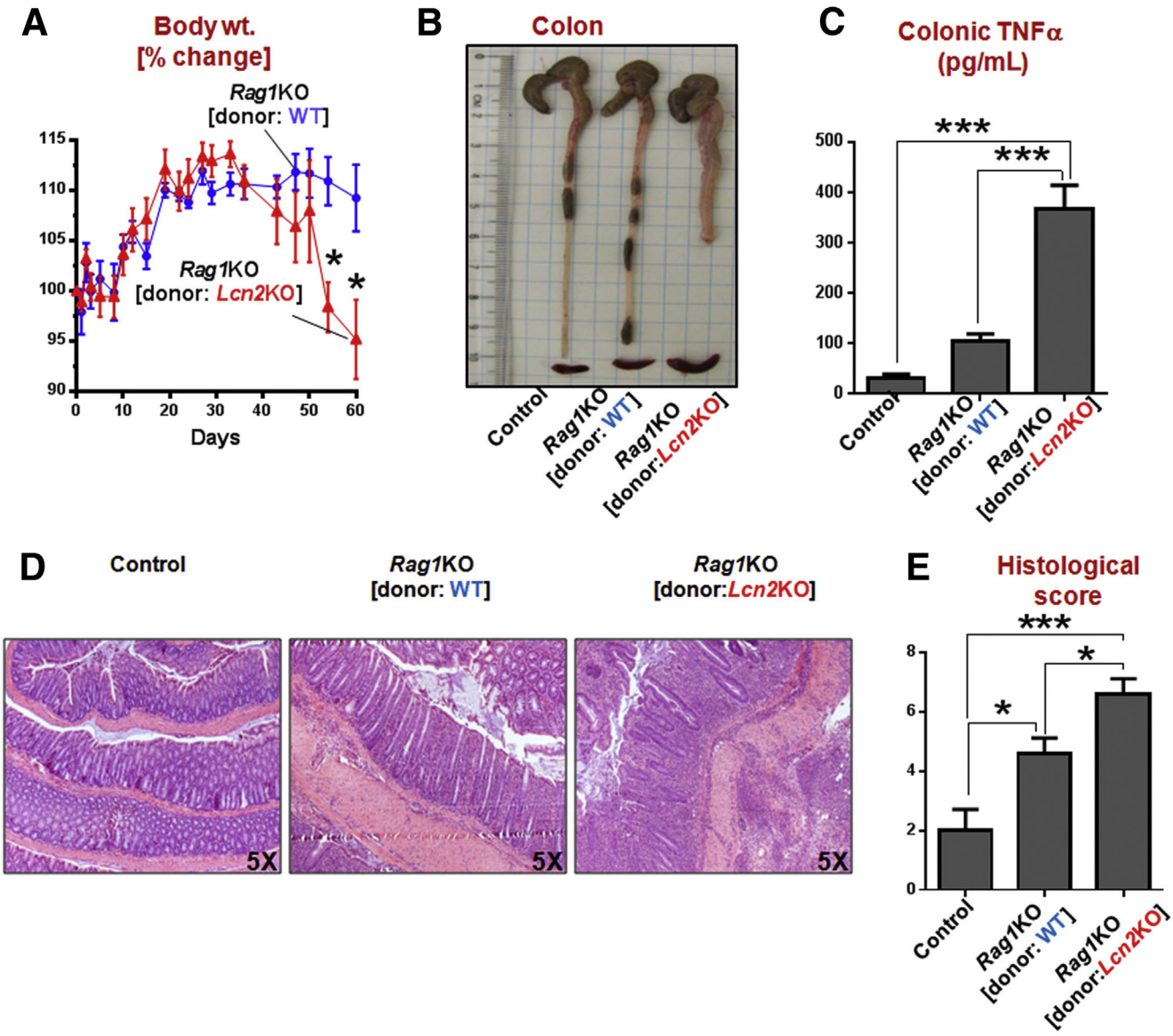

Figure 4. Lcn2-deficient effector T cells are highly colitogenic in *Rag1*KO mice. Four-week-old female *Rag1*KO (n = 5) were given $CD4^+CD25^-$ cells (0.5×10^6 cells/mouse intravenously, sorted via flow cytometry) from *Lcn2*KO or their WT littermates and disease pathogenesis was monitored. (*A*) Body weight, (*B*) gross colon, and (*C*) TNFα in ex vivo colon cultures. (*D*) H&E-stained colons of *Rag1*KO control, WT recipients, and *Lcn2*KO recipients, and the (*E*) corresponding histologic score. Results are expressed as means ± SEM. (*A*, *C*, and *E*) Unpaired *t* test and (*C* and *E*) the 1-way analysis of variance with the Dunnett multiple comparison test were used. $P < .05$ was considered statistically significant. $^*P < .05$ and $^{***}P < .001$.

injections of αIL10R. Remarkably, gut sterilization by antibiotics substantially ameliorated colitis in *Lcn2*KO mice (Supplementary Figure 7). Antibiotic-treated *Lcn2*KO mice showed less body weight loss, relatively smaller mesenteric lymph nodes, normal colon length, and reduced spleen weight, cecum and colon weight, and serum keratinocyte-derived chemokine (Supplementary Figure 7*A*–*G*). In addition, immune cell infiltration and colonic inflammation also were reduced substantially in antibiotic-treated *Lcn2*KO mice (Supplementary Figure 7*H*–*J*).

To further investigate the extent to which *Lcn2*KO mice harbor colitogenic microbiota, *Lcn2*KO or WT littermates mice were co-housed (CoH) with the colitis-prone *Il10*KO mice, the latter were monitored for the development of spontaneous colitis. Herein, *Il10*KO mice will be referred as *Lcn2*KO-CoH and WT-CoH to correspond to the strains of co-housed mice. *Lcn2*KO-CoH mice initially gained less body weight compared with WT-CoH mice, but the body weight loss became more apparent after 3 weeks (Figure 6*A*). After 6 weeks, approximately 50% of *Lcn2*KO-CoH mice developed rectal prolapse (data not shown). Notably, approximately 80% of *Lcn2*KO-CoH mice showed rectal prolapse by 8 weeks with concomitant splenomegaly and colomegaly (Figure 6*B*–*D*). In comparison, no rectal prolapse was observed in WT-CoH mice throughout the duration of this study. Collectively, these results suggest that *Lcn2*KO mice

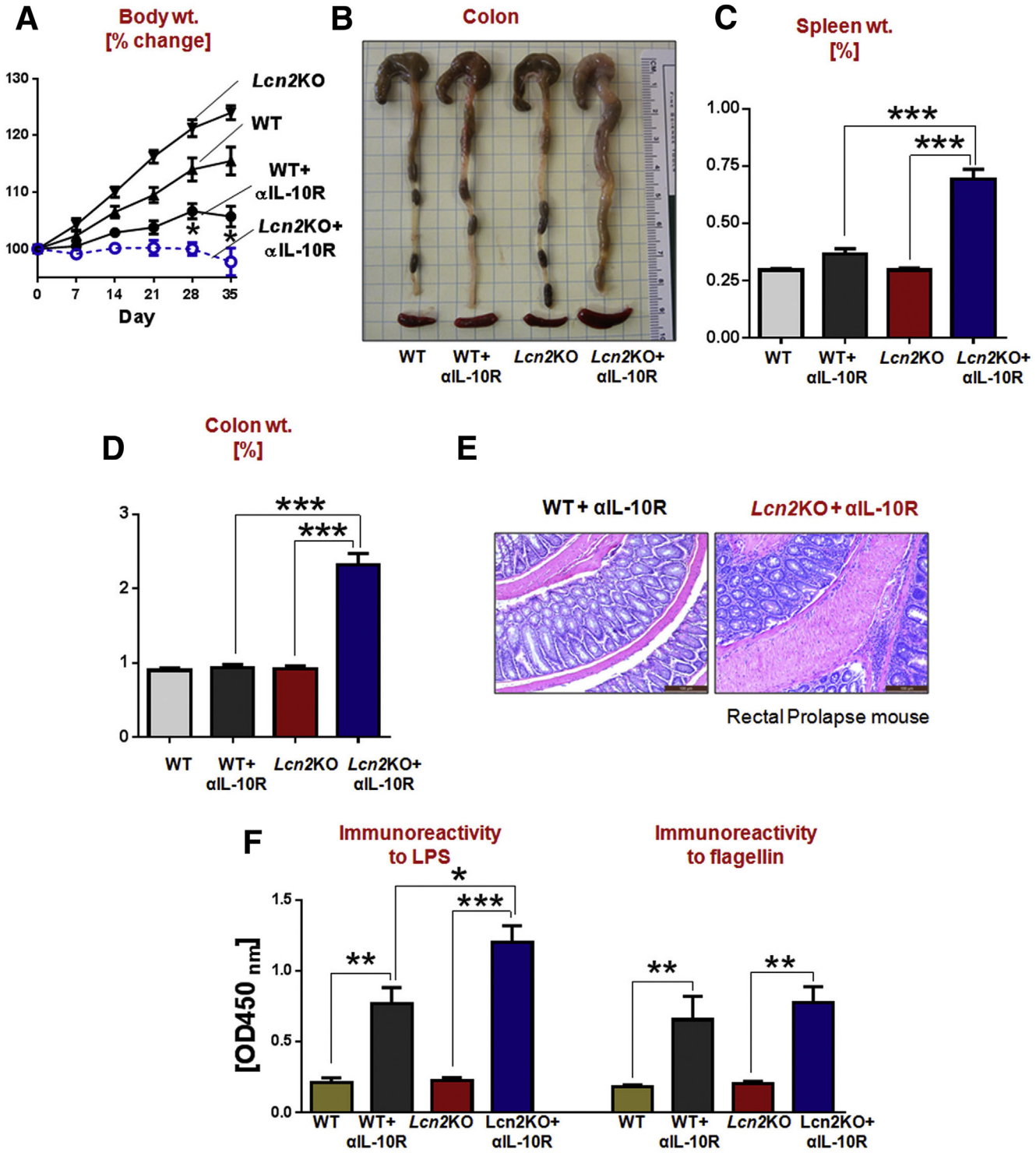

Figure 5. *Lcn2*KO mice develop severe IBD upon IL10R neutralization. Six-week-old male *Lcn2*KO mice and their WT littermates (n = 4-6) were treated with IL10R-neutralizing antibody (1.0 mg/mouse, intraperitoneally, weekly) for up to 4 weeks. One week after the last (fourth) injection, mice were euthanized and analyzed for standard colitis parameters. (*A*) Body weight, (*B*) gross pictures of colon and spleen (*lower panel*), (*C*) spleen weight, (*D*) colon weight, and (*E*) H&E-stained colon sections. (*F*) *Bar graphs* represent immunoreactivity to LPS and flagellin in the serum samples obtained from control and αIL10R-treated WT and *Lcn2*KO mice. Results are expressed as means ± SEM. (*A*) Unpaired *t* test and (*C*, *D*, and *F*) 1-way analysis of variance with the Tukey multiple comparison test were used. $P < .05$ was considered statistically significant. *$P < .05$, **$P < .01$, and ***$P < .001$.

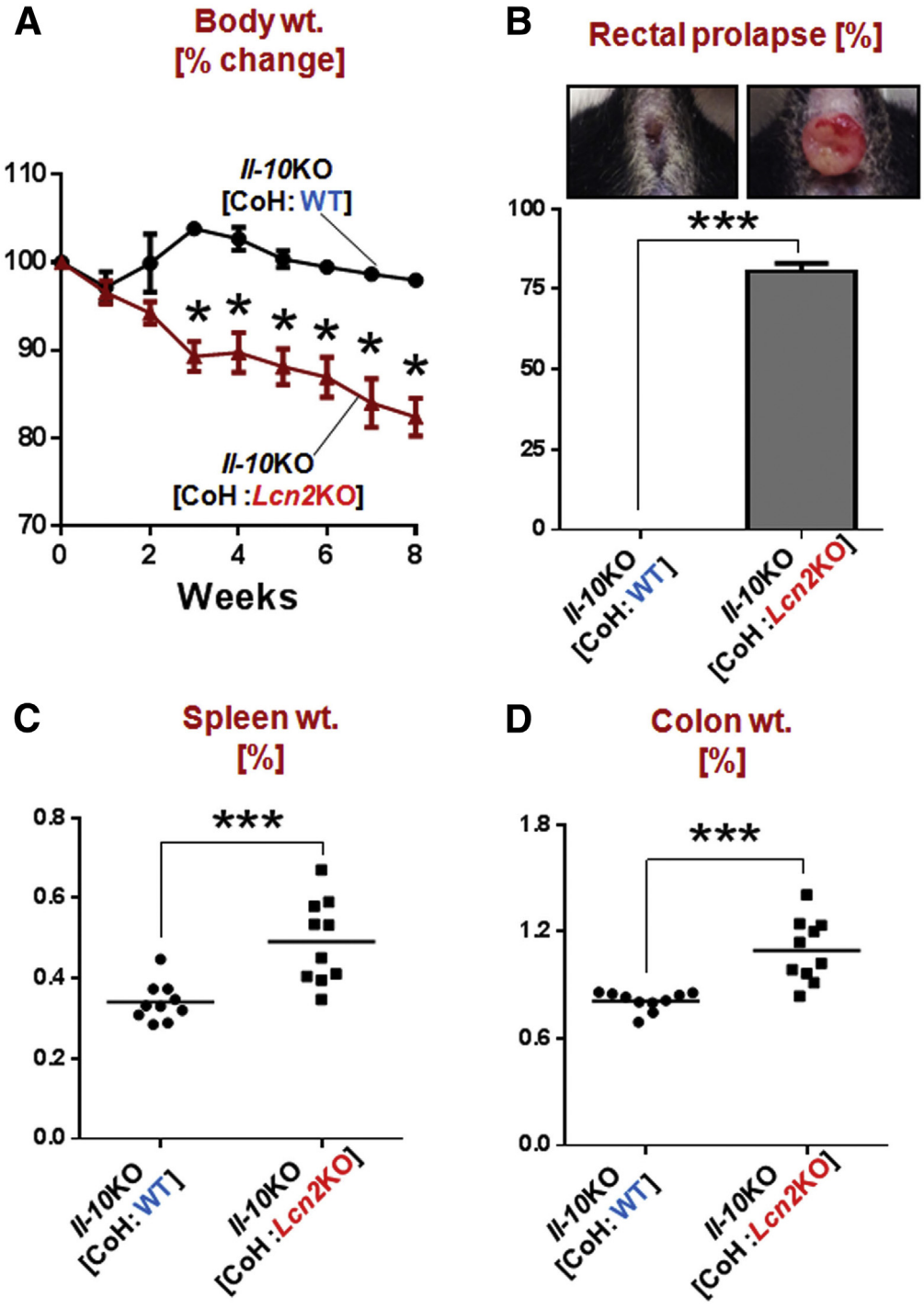

Figure 6. Accelerated spontaneous colitis in *Il10*KO mice co-housed with *Lcn2*KO mice. Immediately after weaning (21 days), male *Lcn2*KO, WT, and *Il10*KO mice (n = 10) were co-housed and monitored for body weight, sticky stools, and rectal prolapse as the end point. (*A*) *Line graph* shows the percentage change in the body weight of *Il10*KO mice CoH with WT or *Lcn2*KO mice. (*B*) Mice were observed continuously for up to 8 weeks for the development of rectal prolapse. After 8 weeks the mice were euthanized and analyzed for colitic parameters. *Bar graphs* represent the (*C*) spleen weight and (*D*) colon weight. Results are expressed as means ± SEM. (*A–C* and *E*) An unpaired *t* test was used. $P < .05$ was considered statistically significant. *$P < .05$ and ***$P < .001$.

harbor not only quantitatively more and distinct microbial community in the gut, but a colitogenic microbiota that is transmissible and can exacerbate spontaneous colitis in susceptible hosts such as *Il10*KO mice.

Discussion

During IBD, the host expresses a plethora of proinflammatory (eg, TNFα) and anti-inflammatory (eg, IL10) molecules, accompanied by APPs, wherein the latter represent a presumed attempt to restore immunologic equilibrium. One such APP, Lcn2, which belongs to a family of small secreted glycoproteins, confers several physiological functions: controlling gut bacterial overgrowth and promoting mucosal regeneration and tissue repair, which can modulate gut health. By using bone marrow chimeric mice, we further confirmed that nonimmune cells, possibly IECs[47] and hepatocytes,[57] contribute the majority of systemic Lcn2 during

the normal and inflamed states. To a lesser extent, the levels of circulating Lcn2 also are contributed by immune cells, particularly neutrophils that express and store rich amounts of Lcn2 in their granules.[13,58] Colocalization of Lcn2 with immune cells in the inflamed colon suggests that immune cells clearly contribute to increased intestinal Lcn2 upon DSS-induced inflammation, although future studies will be needed to determine the role of such Lcn2 in regulating gut inflammation. We further showed that, in vivo, Lcn2 expression is regulated by gut microbiota and in a partial MyD88-dependent fashion. Although the data presented here point prominently to MyD88 signaling being required for Lcn2 production in the inflamed colon, it should be acknowledged that MyD88-dependent signaling may not account solely for the release of Lcn2 in the colon during colitis. However, there is a possibility that other signaling pathways, which are not examined in the present study, also may contribute to the induction of Lcn2 during IBD.

Intriguingly, the absence of Lcn2 led to the increase of procolitogenic factors, which include increased colonic bacterial adhesive proteins, gut bacterial burden, and expansion of *Bacteroidetes*. Accordingly, both acute and chronic colitis were exacerbated and more pronounced in mice lacking *Lcn2*. Gut sterilization and co-housing experiments further suggest that the exacerbated colitis in *Lcn2*KO mice could be the result of their gut microbiota dysbiosis. Collectively, our study suggests that Lcn2 could play a key role in maintaining a healthy gut microbiota composition, thus reducing the susceptibility to develop colitis.

Neutrophils play a critical role in maintaining intestinal homeostasis as appropriate, and timely mucosal neutrophil infiltration is needed for proper initiation, perpetuation, and resolution of inflammation. Published reports have indicated that Lcn2 facilitates neutrophil recruitment at the inflammatory site by inducing IL8, a bona fide chemotactic agent.[19,26,59] Moreover, Lcn2 itself is an indispensable factor for neutrophil adhesion, migration, and function.[26] Accordingly, mice lacking Lcn2 show reduced neutrophil infiltration and colonic MPO activity in response to intestinal inflammation. The impaired neutrophil infiltration in *Lcn2*KO mice may compromise neutrophil-mediated defense against bacterial overgrowth and also potentially impair the recruitment of other immune cells that are necessary to promote mucosal healing.[56] However, excessive recruitment of immune cells also could result in acute flares of IBD.[56] A recent study showed that junctional adhesion molecule-like protein, which is derived from neutrophils, inhibits wound repair by reducing epithelial proliferation.[60] Thus, during intestinal inflammation, neutrophil functions can be viewed as a double-edged sword that keeps gut bacteria in check and helps in mucosal repair, whereas uncontrolled neutrophil infiltration may result in IBD flares and worsen the IBD.

Lcn2 has been reported to mediate both anti-inflammatory or proinflammatory functions depending on the circumstances. In various acute and chronic inflammatory disorders, the significantly increased levels of Lcn2 are shown to perform several key anti-inflammatory functions: supporting the M2 macrophage phenotype switch[28] that promotes wound healing and fibrosis,[61] inducing the anti-inflammatory cytokine IL10 by macrophages,[28] serving as a survival factor[22] (which favors ulcer healing), promoting cell migration and wound repair,[62] acting as an endogenous inhibitor of inflammation,[63] and controlling gut bacterial overgrowth by preventing its iron uptake.[23] Furthermore, increased proinflammatory and procolitogenic responses are observed in immune cells lacking Lcn2.[18,64] Accordingly, we also observed a heightened colitogenic capacity of Lcn2-deficient T cells ($CD4^+CD25^-$) upon their transfer into recipient *Rag1*KO mice. Altogether, gut bacterial dysbiosis, dysregulated immune cell response, and compromised repair mechanisms during Lcn2 deficiency could increase the likelihood of *Lcn2*KO mice to develop colitis.

However, on the flip side, several studies also have reported the proinflammatory aspect of Lcn2, as follows: (1) it induces proinflammatory signaling in Alzheimer's disease,[65] (2) siderophore-bound Lcn2 induces the release of proinflammatory IL8 and IL6 from epithelial cells,[20,66] and (3) the absence of Lcn2 protects against Salmonella enterica serovar Typhimurium-induced colitis in mice.[67] Further mechanistic studies are warranted to elucidate the proinflammatory vs the anti-inflammatory properties of Lcn2 and explore whether Lcn2 could be exploited as a therapeutic target for IBD.

The healthy human gut predominantly harbors *Firmicutes* (~64%) and *Bacteroidetes* (~23%), the other 2 phyla are *Proteobacteria* (~8%) and *Actinobacteria* (~3%).[68] Gut bacterial dysbiosis has been associated with IBD[68–70] and, in particular, the expansion of *Proteobacteria* is known to be correlated positively with the severity of IBD in both mice and human beings.[69,71] Among its multifaceted functions, Lcn2 is known to exert antimicrobial pressure on bacterial growth by chelating bacterial siderophore and limiting bacterial acquisition of iron. Recently, we showed that Lcn2 mediates an additional function to preserve MPO activity by preventing its inactivation by prototypical bacterial siderophore enterobactin produced by the opportunistic pathogen *Escherichia coli*.[27] The present study highlights that aggravated colitis in mice lacking Lcn2 could be, at least in part, microbiota-dependent. Accordingly, Lcn2-deficient mice showed increased gut microbiotal load and altered microbial community, characterized by significant expansion of *Bacteroidetes*, and, to a lesser extent, *Proteobacteria*. Increased microbiota reflect an increased pool of bacterial products (eg, lipopolysaccharide and flagellin) and/or toxic metabolites (trimethylamine N-oxide and taurocholate) at levels that continuously insult the gut and deteriorate the mucosal barrier. Previously, we showed that Lcn2-deficient mice are highly susceptible to bacterial and LPS-induced sepsis.[18] In support of this notion, we observed exacerbated colitis in *Lcn2*KO mice, suggesting a salient role of gut microbiota in IBD pathogenesis. The mitigated colitis phenotype in microbiota-ablated *Lcn2*KO mice and the increased incidence of rectal prolapse in *Il10*KO mice when co-housed with *Lcn2*KO further support our hypothesis that microbiota play a key role in IBD pathogenesis in *Lcn2*KO mice. Intriguingly, the profound up-regulation of Lcn2 expression was observed in colonic tissue of patients with active IBD.[47] It is plausible that increased levels of human

Lcn2 can help to suppress the overgrowth of *E coli*, known to be associated with IBD flares, and induce overall changes in the bacterial community, which could mitigate the symptoms of IBD. Therefore, it would be interesting to examine whether enhanced Lcn2 could regulate the gut microbiota during active ulcerative colitis or active Crohn's disease in human beings. Furthermore, we envision future studies that evaluate which form (monomeric vs dimeric) and source (immune vs nonimmune) of Lcn2 is important, which would advance our current understanding on the role of Lcn2 during IBD.

Lcn2 has emerged in recent years as a biomarker of several acute and chronic inflammatory diseases including IBD.[8,13,72] Indeed, mucosal Lcn2 often is increased in patients with IBD[32] and in colitic mice.[8] In the present study, we show that Lcn2 is a microbiota-induced and MyD88-dependent protein in the gut; deficiency of Lcn2 aggravates both acute and chronic colitis in mice. Microbiota ablation diminished the colitis in *Lcn2*KO mice whereas an increased incidence of rectal prolapse in *Il10*KO mice was observed when co-housed with *Lcn2*KO mice, suggesting that *Lcn2*KO mice carry a microbiota with colitogenic property. Collectively, we showed that Lcn2 is not just a biomarker of gut inflammation, but its up-regulation protects against IBD by controlling, in part, gut bacterial dysbiosis and proper neutrophil infiltration. Thus, Lcn2, similar to its human ortholog NGAL, a small protein with a simple structure and high structural plasticity, may be a promising therapeutic agent to treat human IBD.

References

1. Ananthakrishnan AN. Epidemiology and risk factors for IBD. Nat Rev Gastroenterol Hepatol 2015;12:205–217.
2. Morgan XC, Tickle TL, Sokol H, et al. Dysfunction of the intestinal microbiome in inflammatory bowel disease and treatment. Genome Biol 2012;13:R79.
3. Jostins L, Ripke S, Weersma RK, et al. Host-microbe interactions have shaped the genetic architecture of inflammatory bowel disease. Nature 2012;491:119–124.
4. Campbell CA, Walker-Smith JA, Hindocha P, et al. Acute phase proteins in chronic inflammatory bowel disease in childhood. J Pediatr Gastroenterol Nutr 1982; 1:193–200.
5. Janas RM, Ochocinska A, Snitko R, et al. Neutrophil gelatinase-associated lipocalin (NGAL) in blood in children with inflammatory bowel disease. J Gastroenterol Hepatol 2014;29:1883–1889.
6. Nielsen BS, Borregaard N, Bundgaard JR, et al. Induction of NGAL synthesis in epithelial cells of human colorectal neoplasia and inflammatory bowel diseases. Gut 1996; 38:414–420.
7. Vijay-Kumar M, Sanders CJ, Taylor RT, et al. Deletion of TLR5 results in spontaneous colitis in mice. J Clin Invest 2007;117:3909–3921.
8. Chassaing B, Srinivasan G, Delgado MA, et al. Fecal lipocalin 2, a sensitive and broadly dynamic non-invasive biomarker for intestinal inflammation. PLoS One 2012; 7:e44328.
9. Viau A, El Karoui K, Laouari D, et al. Lipocalin 2 is essential for chronic kidney disease progression in mice and humans. J Clin Invest 2010;120:4065–4076.
10. Yang J, Mori K, Li JY, et al. Iron, lipocalin, and kidney epithelia. Am J Physiol Renal Physiol 2003;285:F9–F18.
11. Mishra J, Dent C, Tarabishi R, et al. Neutrophil gelatinase-associated lipocalin (NGAL) as a biomarker for acute renal injury after cardiac surgery. Lancet 2005; 365:1231–1238.
12. Rodvold JJ, Mahadevan NR, Zanetti M. Lipocalin 2 in cancer: when good immunity goes bad. Cancer Lett 2012;316:132–138.
13. Chakraborty S, Kaur S, Guha S, et al. The multifaceted roles of neutrophil gelatinase associated lipocalin (NGAL) in inflammation and cancer. Biochim Biophys Acta 2012; 1826:129–169.
14. Goetz DH, Holmes MA, Borregaard N, et al. The neutrophil lipocalin NGAL is a bacteriostatic agent that interferes with siderophore-mediated iron acquisition. Mol Cell 2002;10:1033–1043.
15. Devireddy LR, Hart DO, Goetz DH, et al. A mammalian siderophore synthesized by an enzyme with a bacterial homolog involved in enterobactin production. Cell 2010; 141:1006–1017.
16. Bao GH, Xu J, Hu FL, et al. EGCG inhibit chemical reactivity of iron through forming an Ngal-EGCG-iron complex. Biometals 2013;26:1041–1050.
17. Bao G, Clifton M, Hoette TM, et al. Iron traffics in circulation bound to a siderocalin (Ngal)-catechol complex. Nat Chem Biol 2010;6:602–609.
18. Srinivasan G, Aitken JD, Zhang B, et al. Lipocalin 2 deficiency dysregulates iron homeostasis and exacerbates endotoxin-induced sepsis. J Immunol 2012; 189:1911–1919.
19. Nelson AL, Ratner AJ, Barasch J, et al. Interleukin-8 secretion in response to aferric enterobactin is potentiated by siderocalin. Infect Immun 2007;75:3160–3168.
20. Bachman MA, Miller VL, Weiser JN. Mucosal lipocalin 2 has pro-inflammatory and iron-sequestering effects in response to bacterial enterobactin. PLoS Pathog 2009; 5:e1000622.
21. Hu L, Hittelman W, Lu T, et al. NGAL decreases E-cadherin-mediated cell-cell adhesion and increases cell motility and invasion through Rac1 in colon carcinoma cells. Lab Invest 2009;89:531–548.
22. Tong Z, Wu X, Ovcharenko D, et al. Neutrophil gelatinase-associated lipocalin as a survival factor. Biochem J 2005;391:441–448.
23. Flo TH, Smith KD, Sato S, et al. Lipocalin 2 mediates an innate immune response to bacterial infection by sequestrating iron. Nature 2004;432:917–921.
24. Allred BE, Rupert PB, Gauny SS, et al. Siderocalin-mediated recognition, sensitization, and cellular uptake of actinides. Proc Natl Acad Sci U S A 2015;112:10342–10347.
25. Guglani L, Gopal R, Rangel-Moreno J, et al. Lipocalin 2 regulates inflammation during pulmonary mycobacterial infections. PLoS One 2012;7:e50052.
26. Schroll A, Eller K, Feistritzer C, et al. Lipocalin 2 ameliorates granulocyte functionality. Eur J Immunol 2012; 42:3346–3357.

27. Singh V, Yeoh BS, Xiao X, et al. Interplay between enterobactin, myeloperoxidase and lipocalin 2 regulates E. coli survival in the inflamed gut. Nat Commun 2015; 6:7113.
28. Warszawska JM, Gawish R, Sharif O, et al. Lipocalin 2 deactivates macrophages and worsens pneumococcal pneumonia outcomes. J Clin Invest 2013; 123:3363–3372.
29. Playford RJ, Belo A, Poulsom R, et al. Effects of mouse and human lipocalin homologues 24p3/lcn2 and neutrophil gelatinase-associated lipocalin on gastrointestinal mucosal integrity and repair. Gastroenterology 2006;131:809–817.
30. de Bruyn M, Arijs I, De Hertogh G, et al. Serum neutrophil gelatinase b-associated lipocalin and matrix metalloproteinase-9 complex as a surrogate marker for mucosal healing in patients with Crohn's disease. J Crohns Colitis 2015;9:1079–1087.
31. Vijay-Kumar M, Wu H, Aitken J, et al. Activation of toll-like receptor 3 protects against DSS-induced acute colitis. Inflamm Bowel Dis 2007;13:856–864.
32. Carlson M, Raab Y, Seveus L, et al. Human neutrophil lipocalin is a unique marker of neutrophil inflammation in ulcerative colitis and proctitis. Gut 2002;50:501–506.
33. Oikonomou KA, Kapsoritakis AN, Theodoridou C, et al. Neutrophil gelatinase-associated lipocalin (NGAL) in inflammatory bowel disease: association with pathophysiology of inflammation, established markers, and disease activity. J Gastroenterol 2012;47:519–530.
34. Vijay-Kumar M, Gentsch JR, Kaiser WJ, et al. Protein kinase R mediates intestinal epithelial gene remodeling in response to double-stranded RNA and live rotavirus. J Immunol 2005;174:6322–6331.
35. Singh V, Kumar M, Yeoh BS, et al. Inhibition of interleukin-10 signaling induces microbiota-dependent chronic colitis in apolipoprotein E deficient mice. Inflamm Bowel Dis 2016;22:841–852.
36. Chassaing B, Aitken JD, Malleshappa M, et al. Dextran sulfate sodium (DSS)-induced colitis in mice. Curr Protoc Immunol 2014;104:unit 15.25.
37. Rakoff-Nahoum S, Paglino J, Eslami-Varzaneh F, et al. Recognition of commensal microflora by toll-like receptors is required for intestinal homeostasis. Cell 2004; 118:229–241.
38. Carvalho FA, Nalbantoglu I, Ortega-Fernandez S, et al. Interleukin-1beta (IL-1beta) promotes susceptibility of Toll-like receptor 5 (TLR5) deficient mice to colitis. Gut 2012;61:373–384.
39. Singh V, Yeoh BS, Carvalho F, et al. Proneness of TLR5 deficient mice to develop colitis is microbiota dependent. Gut Microbes 2015;6:279–283.
40. Ferrier L, Berard F, Debrauwer L, et al. Impairment of the intestinal barrier by ethanol involves enteric microflora and mast cell activation in rodents. Am J Pathol 2006; 168:1148–1154.
41. Sanders CJ, Moore DA 3rd, Williams IR, et al. Both radioresistant and hemopoietic cells promote innate and adaptive immune responses to flagellin. J Immunol 2008; 180:7184–7192.
42. Carvalho FA, Aitken JD, Gewirtz AT, et al. TLR5 activation induces secretory interleukin-1 receptor antagonist (sIL-1Ra) and reduces inflammasome-associated tissue damage. Mucosal Immunol 2011;4:102–111.
43. Singh V, Chassaing B, Zhang L, et al. Microbiota-dependent hepatic lipogenesis mediated by stearoyl CoA desaturase 1 (SCD1) promotes metabolic syndrome in TLR5-deficient mice. Cell Metab 2015;22:983–996.
44. Ziegler TR, Luo M, Estivariz CF, et al. Detectable serum flagellin and lipopolysaccharide and upregulated anti-flagellin and lipopolysaccharide immunoglobulins in human short bowel syndrome. Am J Physiol Regul Integr Comp Physiol 2008;294:R402–R410.
45. Chinen T, Komai K, Muto G, et al. Prostaglandin E2 and SOCS1 have a role in intestinal immune tolerance. Nat Commun 2011;2:190.
46. Edgar RC. Search and clustering orders of magnitude faster than BLAST. Bioinformatics 2010;26:2460–2461.
47. Ostvik AE, Granlund AV, Torp SH, et al. Expression of Toll-like receptor-3 is enhanced in active inflammatory bowel disease and mediates the excessive release of lipocalin 2. Clin Exp Immunol 2013;173:502–511.
48. Martensson J, Xu S, Bell M, et al. Immunoassays distinguishing between HNL/NGAL released in urine from kidney epithelial cells and neutrophils. Clin Chim Acta 2012;413:1661–1667.
49. Araki A, Kanai T, Ishikura T, et al. MyD88-deficient mice develop severe intestinal inflammation in dextran sodium sulfate colitis. J Gastroenterol 2005;40:16–23.
50. Singh B, Su YC, Riesbeck K. Vitronectin in bacterial pathogenesis: a host protein used in complement escape and cellular invasion. Mol Microbiol 2010; 78:545–560.
51. Sakwe AM, Koumangoye R, Goodwin SJ, et al. Fetuin-A ({alpha}2HS-glycoprotein) is a major serum adhesive protein that mediates growth signaling in breast tumor cells. J Biol Chem 2010;285:41827–41835.
52. Lucke K, Miehlke S, Jacobs E, et al. Prevalence of Bacteroides and Prevotella spp. in ulcerative colitis. J Med Microbiol 2006;55:617–624.
53. Nagalingam NA, Kao JY, Young VB. Microbial ecology of the murine gut associated with the development of dextran sodium sulfate-induced colitis. Inflamm Bowel Dis 2011;17:917–926.
54. Hooper LV, Macpherson AJ. Immune adaptations that maintain homeostasis with the intestinal microbiota. Nat Rev Immunol 2010;10:159–169.
55. Hokari R, Kurihara C, Nagata N, et al. Increased expression of lipocalin-type-prostaglandin D synthase in ulcerative colitis and exacerbating role in murine colitis. Am J Physiol Gastrointest Liver Physiol 2011; 300:G401–G408.
56. Fournier BM, Parkos CA. The role of neutrophils during intestinal inflammation. Mucosal Immunol 2012; 5:354–366.
57. Xu MJ, Feng D, Wu H, et al. Liver is the major source of elevated serum lipocalin-2 levels after bacterial infection or partial hepatectomy: a critical role for IL-6/STAT3. Hepatology 2015;61:692–702.

58. Kjeldsen L, Johnsen AH, Sengelov H, et al. Isolation and primary structure of NGAL, a novel protein associated with human neutrophil gelatinase. J Biol Chem 1993; 268:10425–10432.
59. Hammond ME, Lapointe GR, Feucht PH, et al. IL-8 induces neutrophil chemotaxis predominantly via type I IL-8 receptors. J Immunol 1995;155:1428–1433.
60. Weber DA, Sumagin R, McCall IC, et al. Neutrophil-derived JAML inhibits repair of intestinal epithelial injury during acute inflammation. Mucosal Immunol 2014; 7:1221–1232.
61. Murray PJ, Wynn TA. Protective and pathogenic functions of macrophage subsets. Nat Rev Immunol 2011; 11:723–737.
62. Miao Q, Ku AT, Nishino Y, et al. Tcf3 promotes cell migration and wound repair through regulation of lipocalin 2. Nat Commun 2014;5:4088.
63. Eller K, Schroll A, Banas M, et al. Lipocalin-2 expressed in innate immune cells is an endogenous inhibitor of inflammation in murine nephrotoxic serum nephritis. PLoS One 2013;8:e67693.
64. Li B, Alli R, Vogel P, et al. IL-10 modulates DSS-induced colitis through a macrophage-ROS-NO axis. Mucosal Immunol 2014;7:869–878.
65. Naude PJ, Nyakas C, Eiden LE, et al. Lipocalin 2: novel component of proinflammatory signaling in Alzheimer's disease. FASEB J 2012;26:2811–2823.
66. Holden VI, Lenio S, Kuick R, et al. Bacterial siderophores that evade or overwhelm lipocalin 2 induce hypoxia inducible factor 1alpha and proinflammatory cytokine secretion in cultured respiratory epithelial cells. Infect Immun 2014;82:3826–3836.
67. Kundu P, Ling TW, Korecka A, et al. Absence of intestinal PPARgamma aggravates acute infectious colitis in mice through a lipocalin-2-dependent pathway. PLoS Pathog 2014;10:e1003887.
68. Frank DN, St Amand AL, Feldman RA, et al. Molecular-phylogenetic characterization of microbial community imbalances in human inflammatory bowel diseases. Proc Natl Acad Sci U S A 2007;104: 13780–13785.
69. Shin NR, Whon TW, Bae JW. Proteobacteria: microbial signature of dysbiosis in gut microbiota. Trends Biotechnol 2015;33:496–503.
70. Winter SE, Winter MG, Xavier MN, et al. Host-derived nitrate boosts growth of E. coli in the inflamed gut. Science 2013;339:708–711.
71. Carvalho FA, Koren O, Goodrich JK, et al. Transient inability to manage proteobacteria promotes chronic gut inflammation in TLR5-deficient mice. Cell Host Microbe 2012;12:139–152.
72. Stallhofer J, Friedrich M, Konrad-Zerna A, et al. Lipocalin-2 is a disease activity marker in inflammatory bowel disease regulated by IL-17A, IL-22, and TNF-alpha and modulated by IL23R genotype status. Inflamm Bowel Dis 2015;21:2327–2340.

Received December 4, 2015. Accepted March 14, 2016.

Correspondence
Address correspondence to: Matam Vijay-Kumar, PhD, Department of Nutritional Sciences 222, Chandlee Laboratory, The Pennsylvania State University, University Park, Pennsylvania 16802. e-mail: mvk13@psu.edu; fax: (814) 863-6103.

Acknowledgments
Human neutrophils were a kind gift from Professor Charles A. Parkos (Emory University). The authors acknowledge Dr Siyang Zheng (Department of Biomedical Engineering, The Pennsylvania State University) for critical input on immunofluorescence staining data, and the authors thank Jesse Aitken, Gayathri Srinivasan, Alyssa Grube, Nimita H. Fifadara, and Madhu Malleshappa for technical assistance.

Conflicts of interest
The authors disclose no conflicts.

Funding
Supported by National Institutes of Health grants K01 DK083275 and R01 DK097865-01A1 (M.V.-K.), DK061417 and DK083890 (A.T.G), and T32AI07445 (B.S.Y.), and by the Crohn's and Colitis Foundation of America Research Fellowship award (B.C.).

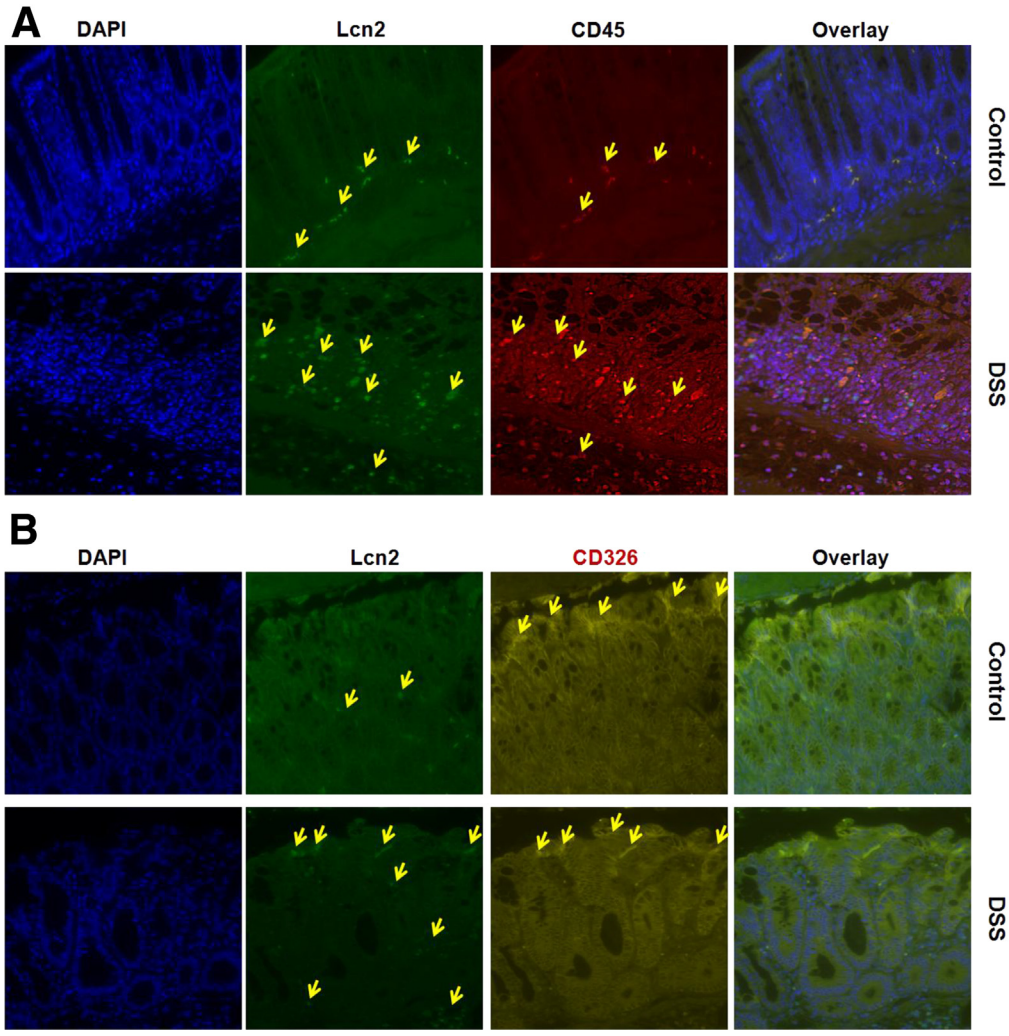

Supplementary Figure 1. Both immune and nonimmune cells contribute in intestinal Lcn2 during colitis. Colonic tissue sections obtained from control and DSS-treated (1.8% in drinking water for up to 7 days) WT mice (n = 4) were processed for immunofluorescence staining with anti-mouse antibodies specific to Lcn2, CD45 (leukocyte marker), and CD326 (epithelial cell adhesion molecule, a marker for epithelial cells). (*A*) Representative images of 4′,6-diamidino-2-phenylindole (DAPI), Lcn2, and CD45 immunostained sections of control (*upper*) and DSS-treated (*lower*) mice. (*B*) Immunofluorescence staining showed Lcn2 and CD326-positive cells in colonic sections from control (*upper*) and DSS-treated (*lower*) mice. Magnification, 400×. *Arrowheads* indicate positive staining.

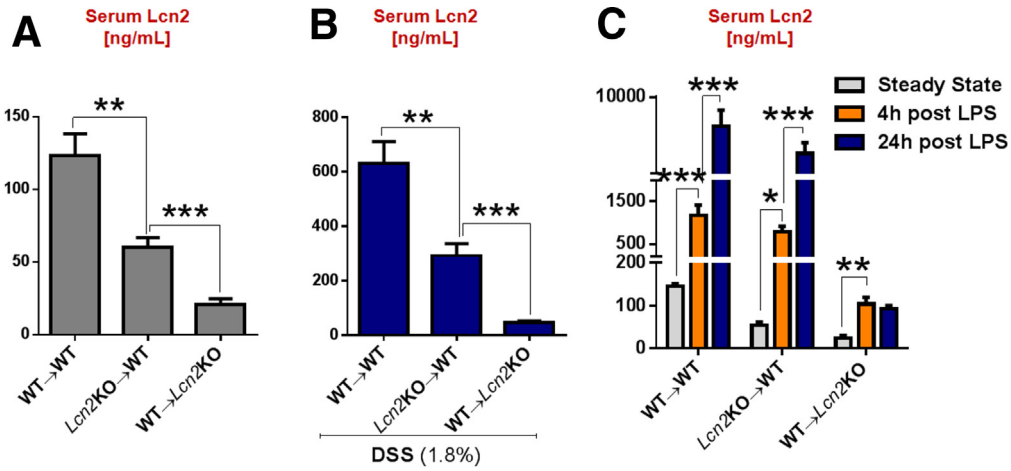

Supplementary Figure 2. Nonimmune cells are principal contributors of circulating Lcn2. To explore the relative contribution of immune and nonimmune cells in maintaining the circulating Lcn2, serum Lcn2 was measured in normal and LPS-stimulated bone marrow chimeric mice (n = 4-5). *Bar graphs* represent serum Lcn2 in (*A*) normal, (*B*) DSS (1.8%) treatment (after 7 days), and (*C*) LPS-treated bone marrow chimeric mice. Results are expressed as means ± SEM. (*A–C*) One-way analysis of variance with the Dunnett multiple comparison test was used. $P < .05$ was considered statistically significant. *$P < .05$, **$P < .01$, and ***$P < .001$.

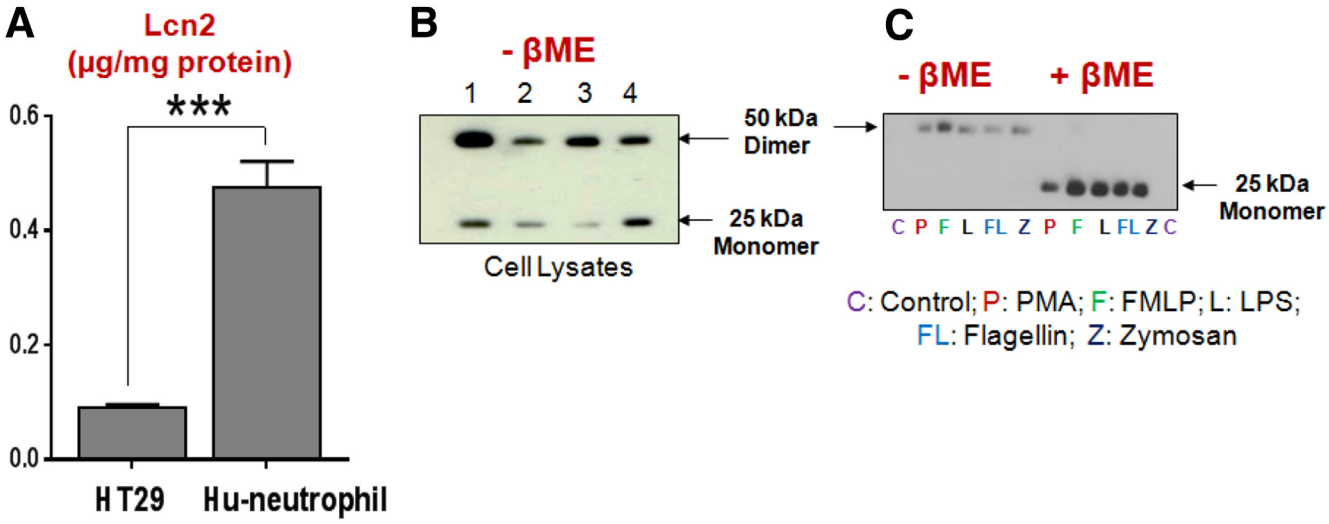

Supplementary Figure 3. Human neutrophils are the richest source of Lcn2. Human neutrophils, obtained from 4 different individuals, and HT29 cells were lysed and analyzed for Lcn2 using ELISA. (A) *Bar graph* represents Lcn2 levels in human neutrophils and HT29 cells. Human neutrophils (2×10^6/well) were stimulated with indicated stimuli in Hank's balanced salt solution for 1 hour at 37°C and Lcn2 was assayed in (*B*) cell lysate and (*C*) cell supernatant by immunoblotting with and without β-mercaptoethanol (βME). Results are expressed as means ± SEM. *$P < .05$. (*A*) An unpaired *t* test was used. $P < .05$ was considered statistically significant. ***$P < .001$.

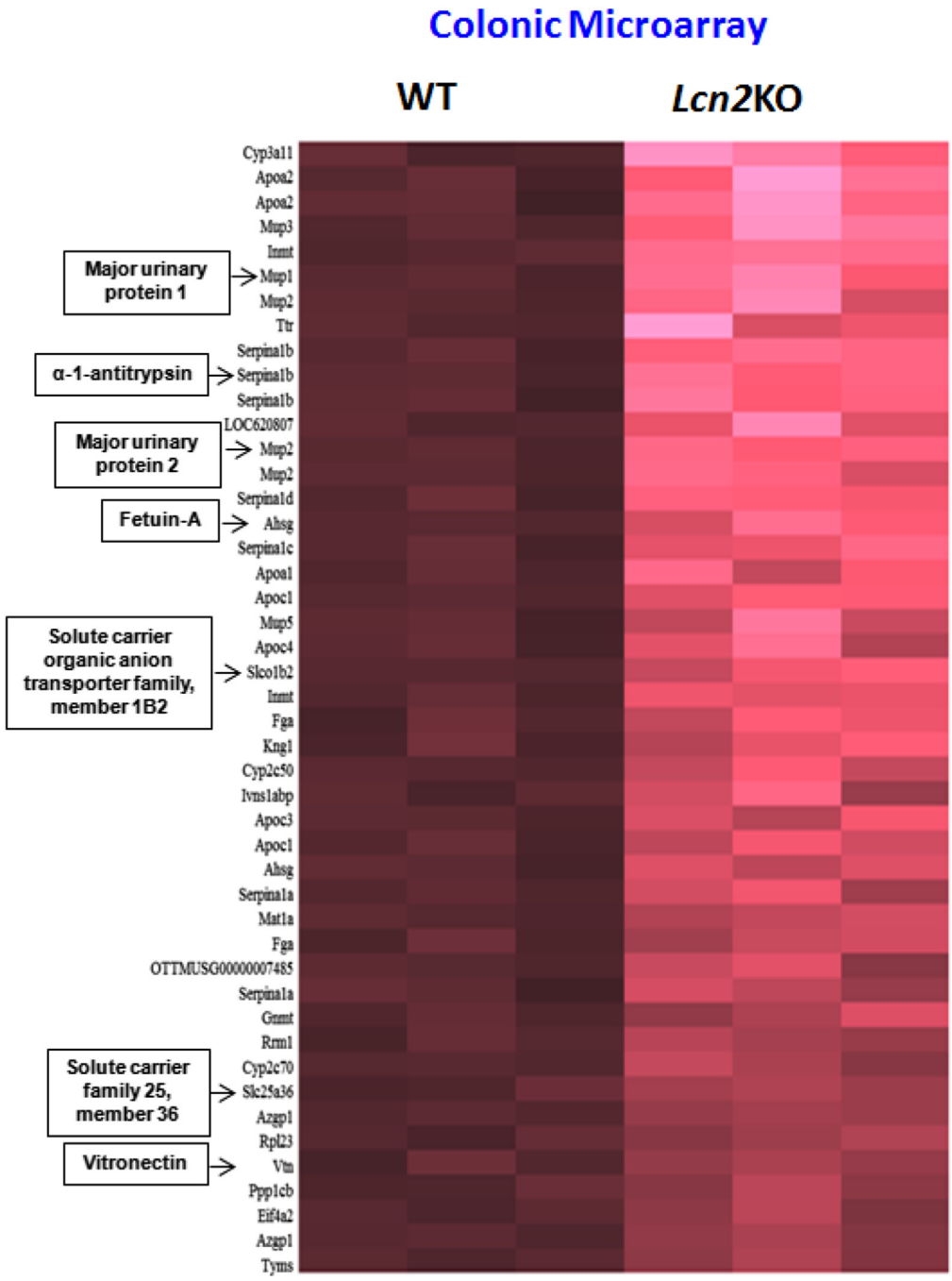

Supplementary Figure 4. Increased colonic expression of bacterial adherence and Lcn2 family genes in mice lacking Lcn2. To examine the global gene expression profile, messenger RNA from colons of 12-week-old male *Lcn2*KO mice and their WT littermates (n = 3) was purified and subjected to microarray analysis. The gene expression heat map of colonic tissue is shown. Pink color shows the increased expression (>1.5-fold) of colonic genes.

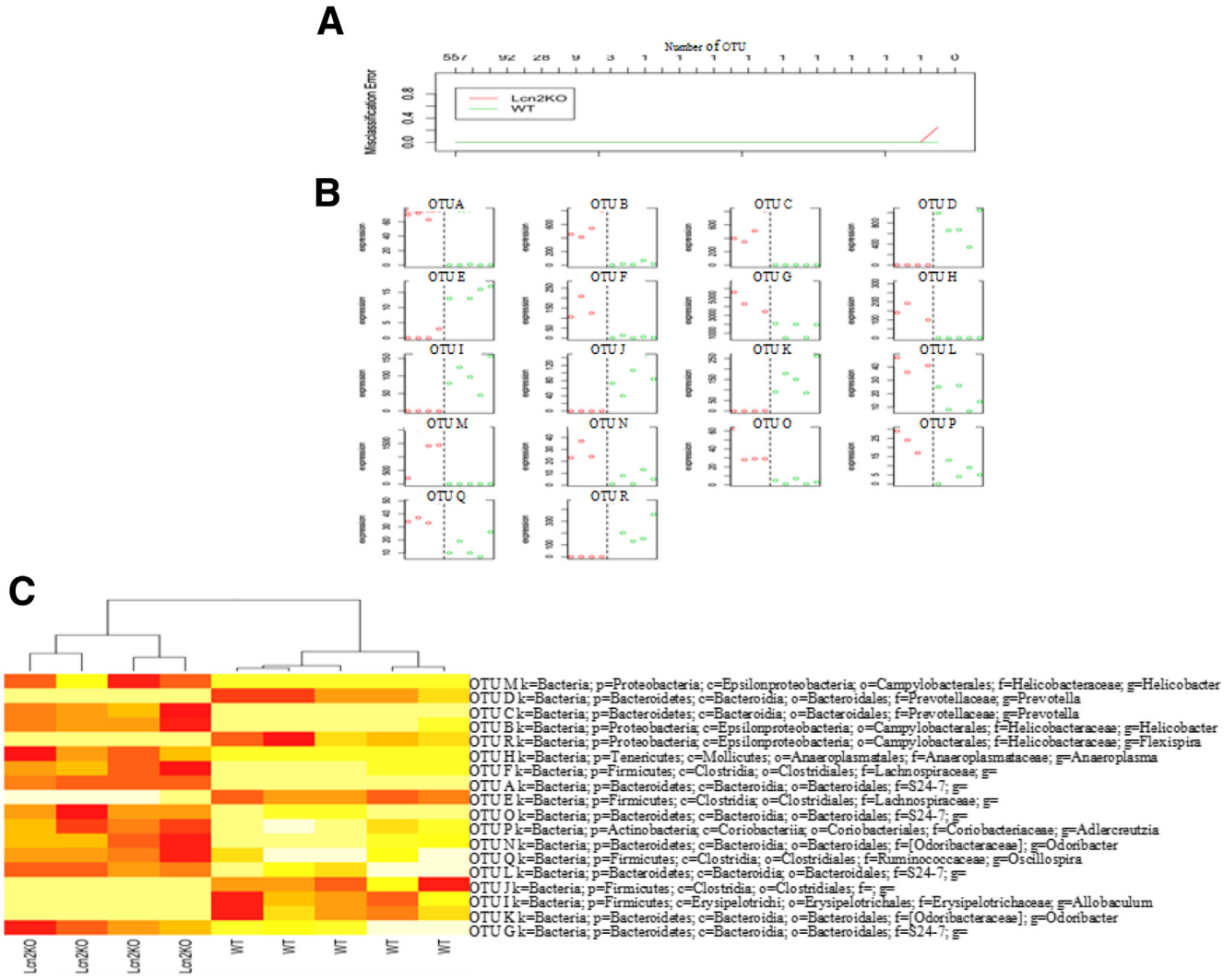

Supplementary Figure 5. Misclassification error rate and heat map representation of the 17 most significantly altered operational taxonomic units (OTUs) in *Lcn2*KO mice. (*A*) Misclassification error rate showing that 17 OTUs were sufficient to discriminate microbiota successfully from each experimental group (WT and *Lcn2*KO, error rate = 0). (*B*) Relative expression of the 17 most significantly altered OTUs in *Lcn2*KO mice compared with WT mice. Green, WT; red, *Lcn2*KO. (*C*) Heat map representation of the 17 most significantly altered OTUs in Lcn2KO mice compared with WT mice. Colors represent the relative expression (white and red for under-represented and overrepresented, respectively). The 17 OTUs are listed on the *right* using their assigned taxonomy, starting with the phylum, then class, order, family, and genus. The dendrogram on the *upper part* represents sample clustering.

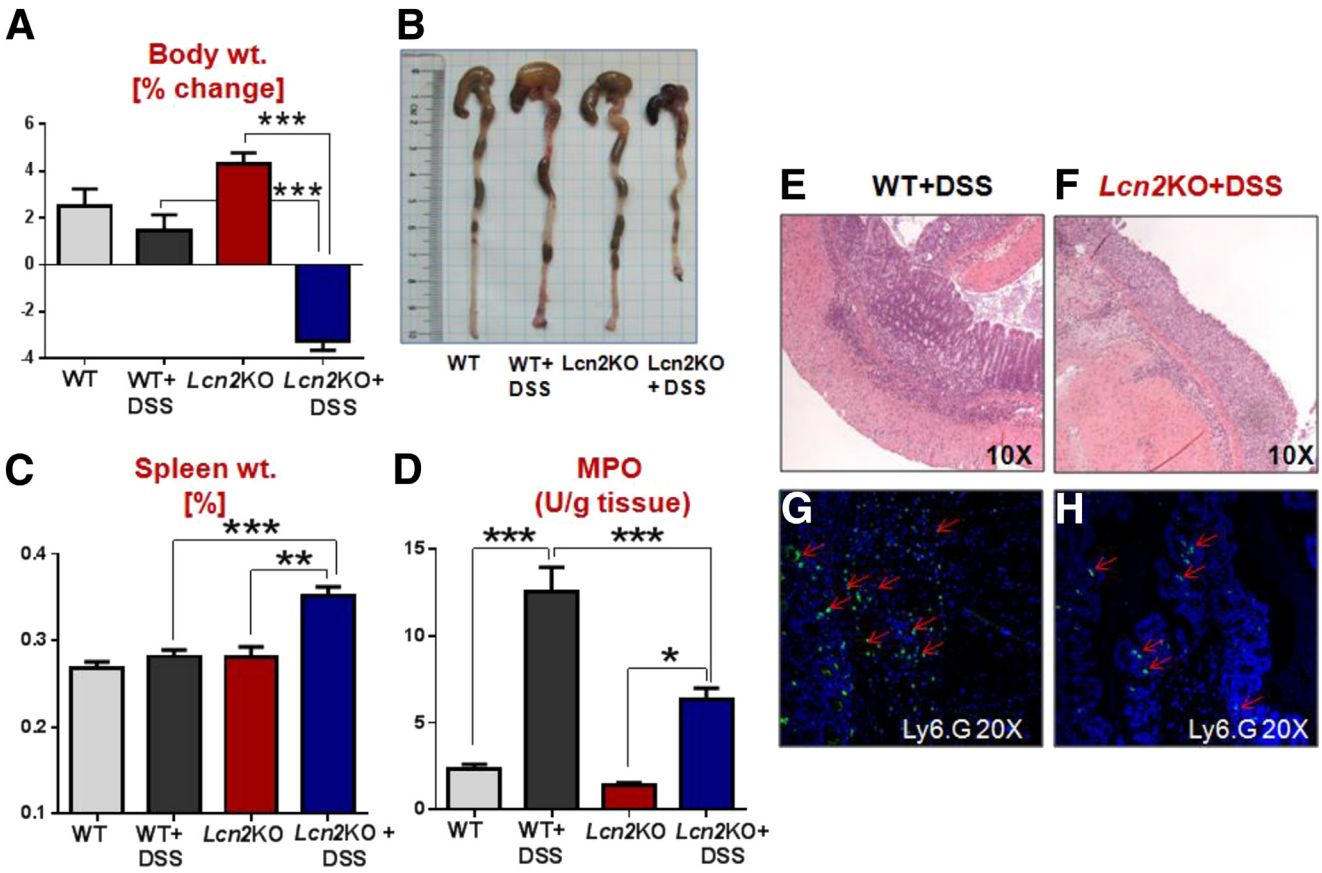

Supplementary Figure 6. Aggravated DSS-induced acute colitis in mice lacking Lcn2. WT and *Lcn2*KO mice (n = 5) were given 1.8% DSS and after 7 days were monitored for (*A*) body weight (*B*) gross colons, (*C*) spleen weight, and (*D*) colonic MPO. H&E-stained colons from (*E*) WT+DSS and (*F*) *Lcn2*KO+DSS mice. Ly-6G–stained colons from (*G*) WT+DSS and (*H*) *Lcn2*KO+DSS mice. Green, Ly6G; blue, 4′,6-diamidino-2-phenylindole. Results are expressed as means ± SEM. **P* < .05. (*A*, *C*, and *D*) One-way analysis of variance with the Tukey multiple comparison test was used. *P* < .05 was considered statistically significant. **P* < .05, ***P* < .01, and ****P* < .001.

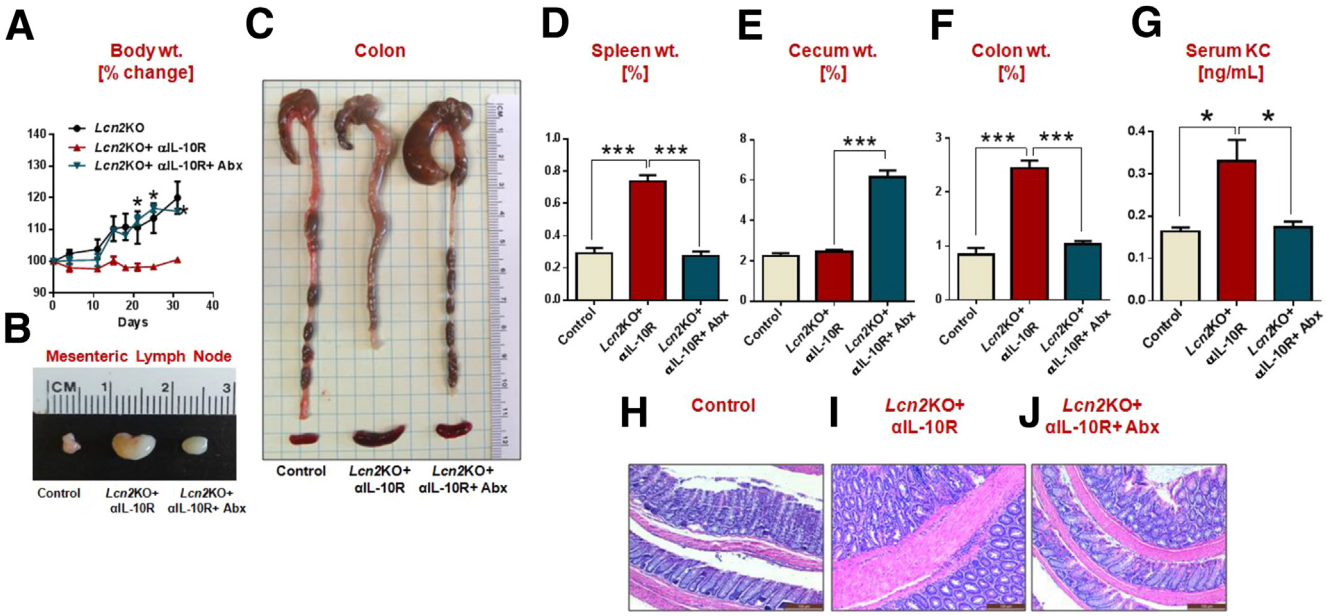

Supplementary Figure 7. Microbiota ablation diminished colitis in anti-IL10R–treated *Lcn2*KO mice. Age-matched male *Lcn2*KO mice (n = 4-6) were maintained on the broad-spectrum antibiotics ampicillin and neomycin in drinking water. After 3 days, mice received α-IL10R mAb (1.0 mg/mouse, intraperitoneally, weekly) for up to 4 weeks and then were analyzed for the development of colitis. (*A*) Body weight, (*B*) mesenteric lymph node, (*C*) gross image of colon, (*D*) spleen weight, (*E*) cecum weight, (*F*) colon weight, (*G*) serum keratinocyte-derived chemokine (KC), and (*H–J*) the H&E-stained sections colonic tissue. Results are expressed as means ± SEM. **P* < .05. (*A*) Unpaired *t* test and (*D*–G) 1-way analysis of variance with the Tukey multiple comparison test were used. *P* < .05 was considered statistically significant. **P* < .05 and ****P* < .001. Abx, antibiotics.